

Interstellar Medium (ISM)

Week 6

2025 April 07 (Monday), 9AM

updated 04/07, 10:35

선광일 (Kwangil Seon)
KASI / UST

Collisionally-Excited Emission Line

- Emission line flux

- In the low density limit, the collisional rate between atoms and electrons is much slower than the (spontaneous) radiative de-excitation rate of the excited level. Thus, we can balance the collisional feeding into level u by the rate of radiative transition back down to level ℓ . The level population is determined by

$$n_e n_\ell k_{\ell u} = A_{u\ell} n_u$$

$$\frac{n_u}{n_\ell} = \frac{n_e k_{\ell u}}{A_{u\ell}}$$

$$= \frac{n_e}{A_{u\ell}} \beta \frac{\langle \Omega_{u\ell} \rangle}{g_\ell} T^{-1/2} \exp\left(-\frac{E_{u\ell}}{kT}\right)$$

where $A_{u\ell}$ is the Einstein coefficient for spontaneous emission. The line emissivity is given by

$$4\pi j_{u\ell} = E_{u\ell} A_{u\ell} n_u = E_{u\ell} n_e n_\ell k_{\ell u}$$

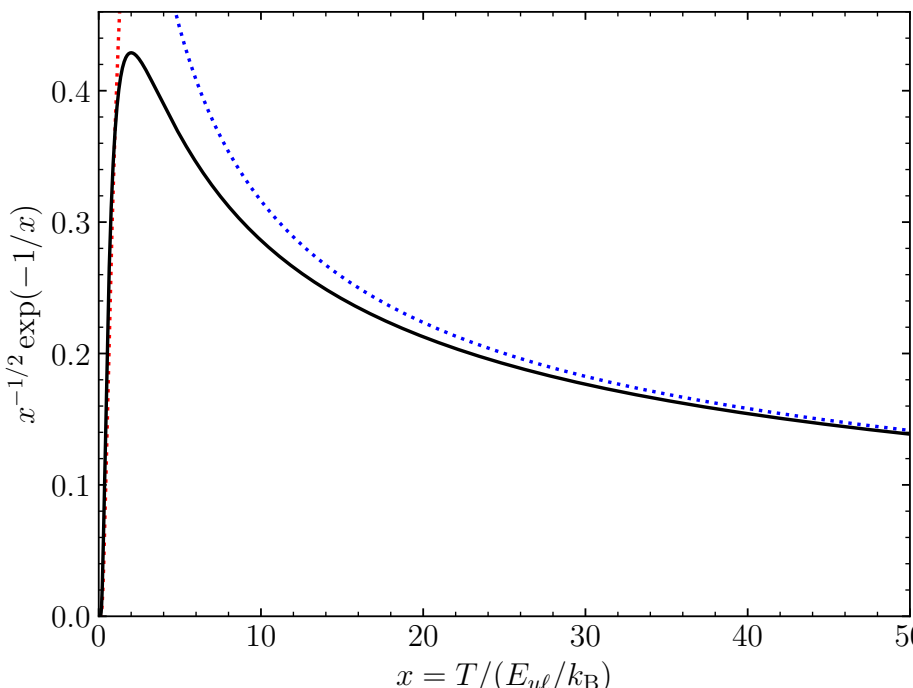
$$= n_e n_\ell E_{u\ell} \frac{8.62942 \times 10^{-6}}{T^{1/2}} \frac{\langle \Omega_{u\ell} \rangle}{g_\ell} \exp\left(-\frac{E_{u\ell}}{kT}\right) \text{ [erg cm}^{-3} \text{ s}^{-1}\text{]}$$

$$\simeq \beta \chi n_e^2 E_{u\ell} T^{-1/2} \frac{\langle \Omega_{u\ell} \rangle}{g_\ell} \exp\left(-\frac{E_{u\ell}}{kT}\right)$$

Here,

$$\beta = \left(\frac{2\pi\hbar^4}{km_e^2}\right)^{1/2} = 8.62942 \times 10^{-6}$$

$$\chi = n_\ell / n_e$$



For low temperature, the exponential term dominates because few electrons have energy above the threshold for collisional excitation, so that the line rapidly fades with decreasing temperature.

At high temperature, the $T^{-1/2}$ term controls the cooling rate, so the line fades slowly with increasing temperature.

- ▶ In **high-density limit**, the level population are set by the Boltzmann equilibrium, and the line emissivity is

$$\frac{n_u}{n_\ell} = \frac{g_u}{g_\ell} \exp\left(-\frac{E_{u\ell}}{kT}\right)$$

$$\begin{aligned} 4\pi j_{u\ell} &= E_{\ell u} A_{u\ell} n_u \\ &= n_\ell E_{\ell u} A_{u\ell} \frac{g_u}{g_\ell} \exp\left(-\frac{E_{\ell u}}{kT}\right) \\ &\simeq \chi n_e E_{\ell u} A_{u\ell} \frac{g_u}{g_\ell} \exp\left(-\frac{E_{\ell u}}{kT}\right) \\ &\rightarrow n_\ell E_{\ell u} A_{u\ell} \frac{g_u}{g_\ell} \quad \text{as } kT \gg E_{\ell u} \end{aligned}$$

Here, the line flux scales as n_e rather than n_e^2 , but the line flux tends to be a constant value at high temperature.

- ▶ **Critical density** is defined as the density where the radiative depopulation rate matches the collisional de-excitation for the excited state.

$$A_{u\ell} n_u = n_e n_u k_{u\ell}$$

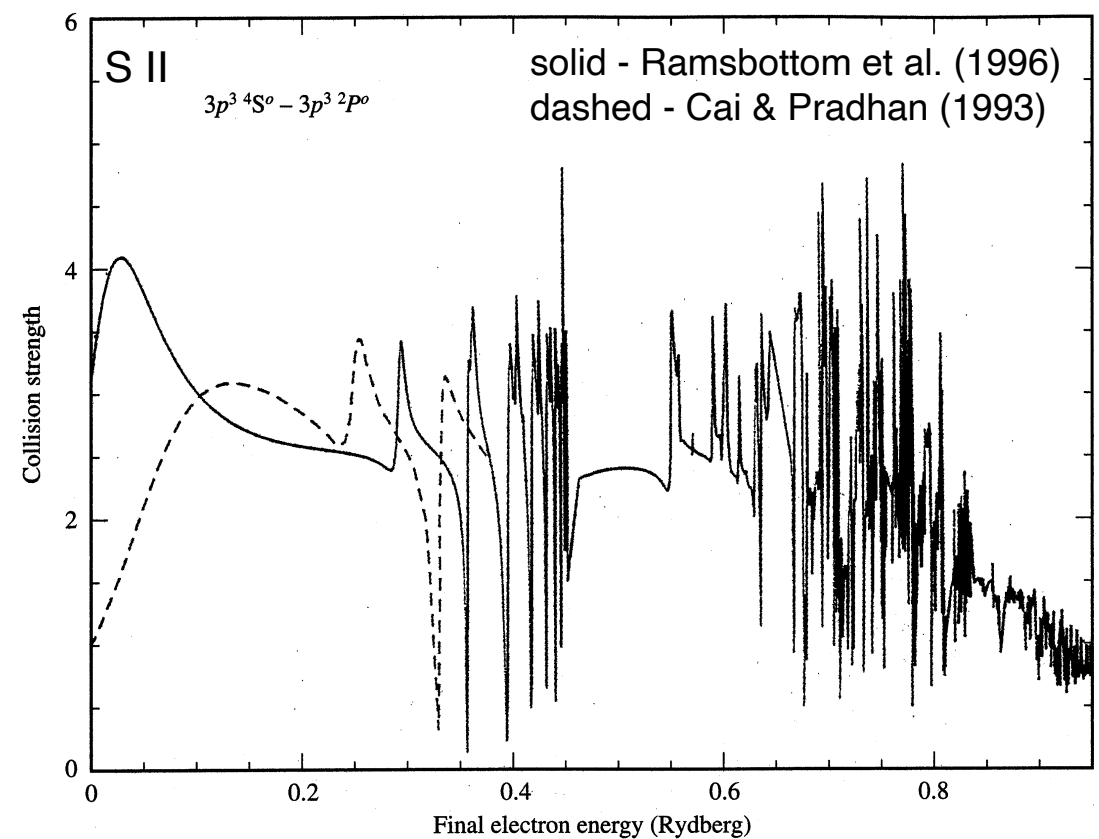
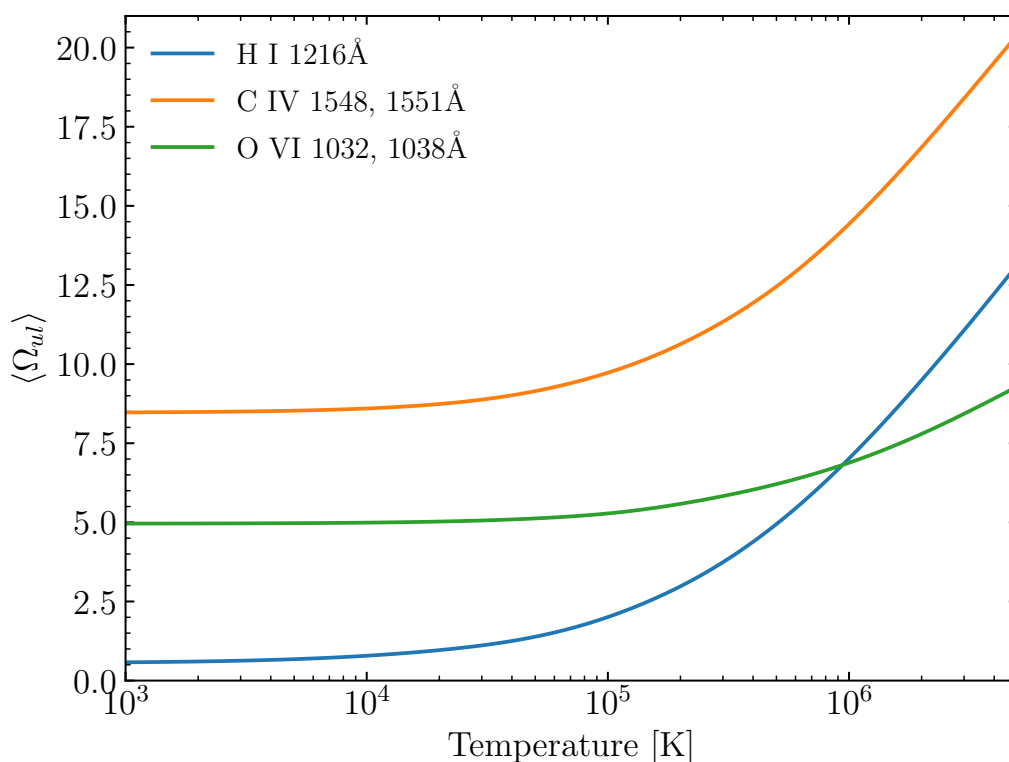
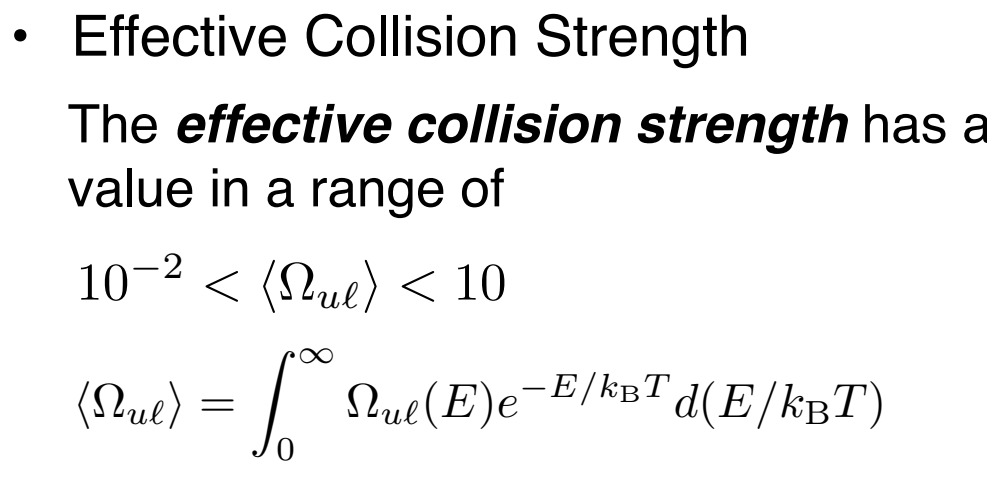
$$n_{\text{crit}} = \frac{A_{u\ell}}{k_{u\ell}}$$

$$\begin{aligned} \rightarrow n_{\text{crit}} &= A_{u\ell} \frac{g_u}{\beta \langle \Omega_{u\ell} \rangle} T^{1/2} \\ &= 1.2 \times 10^3 \frac{A_{u\ell}}{10^{-4} \text{ s}^{-1}} \frac{g_u}{\langle \Omega_{u\ell} \rangle} \left(\frac{T}{10^4 \text{ K}} \right)^{1/2} [\text{cm}^{-3}] \end{aligned}$$

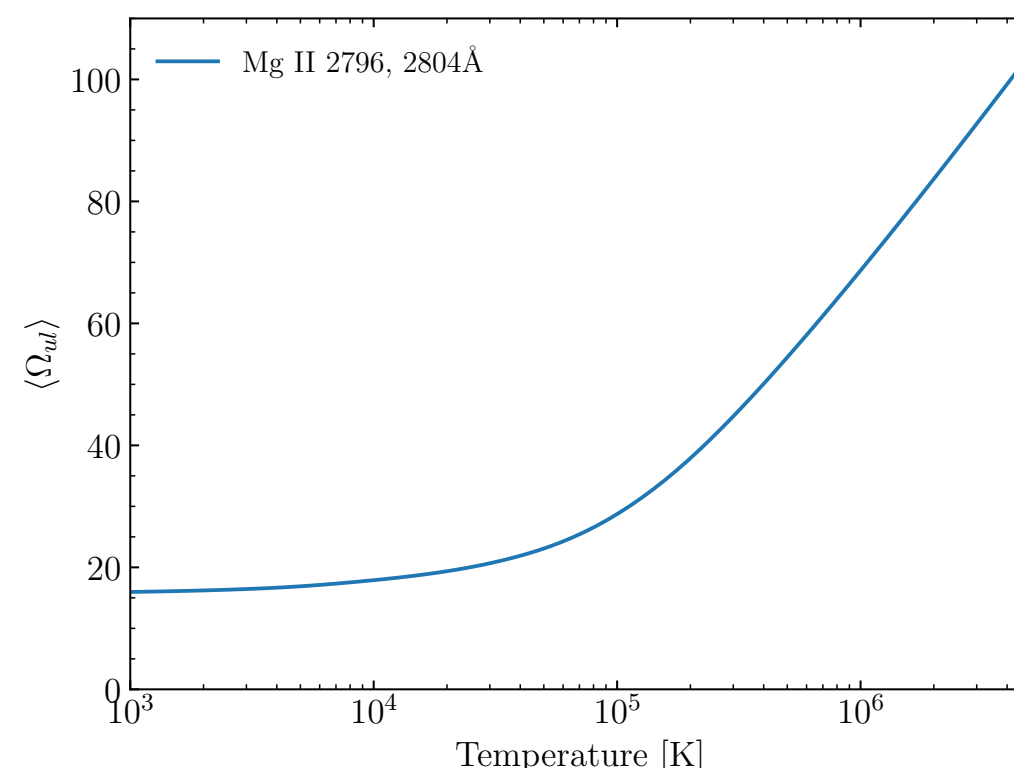
- ▶ At densities higher than the critical density, collisional de-excitation becomes significant, and the forbidden lines will be weaker as the density increases.

At around the critical density, the “line emissivity vs density” plotted in log-log scale changes slope from +2 to +1.

- Collision Strength
 - Quantum mechanical calculations show that (1) the resonance structure in the collision strengths is important and (2) the collision strength increases with energy for neutral species.



Refer to Tables F.1 - F.5 in [Draine]
and the CHIANT atomic database <https://www.chiantidatabase.org/>



- As can be seen in the Tables and the formula, **collisional de-excitation is negligible** for resonance and most forbidden lines in the ISM.

Ion	ℓ	u			$n_{H,\text{crit}}(u)$	
			E_ℓ/k (K)	E_u/k (K)	$\lambda_{u\ell}$ (μm)	$T = 100 \text{ K}$ (cm^{-3})
C II	$^2\text{P}_{1/2}^o$	$^2\text{P}_{3/2}^o$	0	91.21	157.74	2.0×10^3
CI	$^3\text{P}_0$	$^3\text{P}_1$	0	23.60	609.7	620
	$^3\text{P}_1$	$^3\text{P}_2$	23.60	62.44	370.37	720
O I	$^3\text{P}_2$	$^3\text{P}_1$	0	227.71	63.185	2.5×10^5
	$^3\text{P}_1$	$^3\text{P}_0$	227.71	326.57	145.53	8.4×10^3
Si II	$^2\text{P}_{1/2}^o$	$^2\text{P}_{3/2}^o$	0	413.28	34.814	1.0×10^5
Si I	$^3\text{P}_0$	$^3\text{P}_1$	0	110.95	129.68	4.8×10^4
	$^3\text{P}_1$	$^3\text{P}_2$	110.95	321.07	68.473	9.9×10^4
						1.5×10^3

Table 17.1 in [Draine]

- However, it is not true for the 21 cm hyperfine structure line of hydrogen.
 - The critical density for 21cm line is

$$n_{\text{crit}} \sim 10^{-3} (T/100 \text{ K})^{-1/2} [\text{cm}^{-3}]$$

$$A_{u\ell} = 2.88 \times 10^{-15} [\text{s}^{-1}]$$
 - The hyperfine levels are thus essentially in collisional equilibrium in the CNM.

The collisional strengths and other atomic data are available in the CHIANTI atomic database (<https://www.chiantidatabase.org/>).

Ion	Transition l-u	λ μm	A_{ul} s^{-1}	Ω_{ul}	n_{crit} cm^{-3}
C I	$^3\text{P}_0 - ^3\text{P}_1$	609.1354	7.93×10^{-8}	–	(500)
	$^3\text{P}_1 - ^3\text{P}_2$	370.4151	2.65×10^{-7}	–	(3000)
C II	$^2\text{P}_{1/2} - ^2\text{P}_{3/2}$	157.741	2.4×10^{-6}	1.80	47 (3000)
N II	$^3\text{P}_0 - ^3\text{P}_1$	205.3	2.07×10^{-6}	0.41	41
	$^3\text{P}_1 - ^3\text{P}_2$	121.889	7.46×10^{-6}	1.38	256
	$^3\text{P}_2 - ^1\text{D}_2$	0.65834	2.73×10^{-3}	2.99	7700
	$^3\text{P}_1 - ^1\text{D}_2$	0.65481	9.20×10^{-4}	2.99	7700
N III	$^2\text{P}_{1/2} - ^2\text{P}_{3/2}$	57.317	4.8×10^{-5}	1.2	1880
O I	$^3\text{P}_2 - ^3\text{P}_1$	63.184	8.95×10^{-5}	–	$2.3 \times 10^4 (5 \times 10^5)$
	$^3\text{P}_1 - ^3\text{P}_0$	145.525	1.7×10^{-5}	–	$3400 (1 \times 10^5)$
	$^3\text{P}_2 - ^1\text{D}_2$	0.63003	6.3×10^{-3}	–	1.8×10^6
O II	$^4\text{S}_{3/2} - ^2\text{D}_{5/2}$	0.37288	3.6×10^{-5}	0.88	1160
	$^4\text{S}_{3/2} - ^2\text{D}_{3/2}$	0.37260	1.8×10^{-4}	0.59	3890
O III	$^3\text{P}_0 - ^3\text{P}_1$	88.356	2.62×10^{-5}	0.39	461
	$^3\text{P}_1 - ^3\text{P}_2$	51.815	9.76×10^{-5}	0.95	3250
	$^3\text{P}_2 - ^1\text{D}_2$	0.50069	1.81×10^{-2}	2.50	6.4×10^5
	$^3\text{P}_1 - ^1\text{D}_2$	0.49589	6.21×10^{-3}	2.50	6.4×10^5
	$^1\text{D}_2 - ^1\text{S}_0$	0.43632	1.70	0.40	2.4×10^7
Ne II	$^2\text{P}_{1/2} - ^2\text{P}_{3/2}$	12.8136	8.6×10^{-3}	0.37	5.9×10^5
Ne III	$^3\text{P}_2 - ^3\text{P}_1$	15.5551	3.1×10^{-2}	0.60	1.27×10^5
	$^3\text{P}_1 - ^3\text{P}_0$	36.0135	5.2×10^{-3}	0.21	1.82×10^4
Si II	$^2\text{P}_{1/2} - ^2\text{P}_{3/2}$	34.8152	2.17×10^{-4}	7.7	(3.4×10^5)
S II	$^4\text{S}_{3/2} - ^2\text{D}_{5/2}$	0.67164	2.60×10^{-4}	4.7	1240
	$^4\text{S}_{3/2} - ^2\text{D}_{3/2}$	0.67308	8.82×10^{-4}	3.1	3270
S III	$^3\text{P}_0 - ^3\text{P}_1$	33.4810	4.72×10^{-4}	4.0	1780
	$^3\text{P}_1 - ^3\text{P}_2$	18.7130	2.07×10^{-3}	7.9	1.4×10^4
S IV	$^2\text{P}_{1/2} - ^2\text{P}_{3/2}$	10.5105	7.1×10^{-3}	8.5	5.0×10^4
Ar II	$^2\text{P}_{1/2} - ^2\text{P}_{3/2}$	6.9853	5.3×10^{-2}	2.9	1.72×10^6
Ar III	$^3\text{P}_2 - ^3\text{P}_1$	8.9914	3.08×10^{-2}	3.1	2.75×10^5
	$^3\text{P}_1 - ^3\text{P}_0$	21.8293	5.17×10^{-3}	1.3	3.0×10^4
Fe II	$^6\text{D}_{7/2} - ^6\text{D}_{5/2}$	35.3491	1.57×10^{-3}	–	(3.3×10^6)
	$^6\text{D}_{9/2} - ^6\text{D}_{7/2}$	25.9882	2.13×10^{-3}	–	(2.2×10^6)

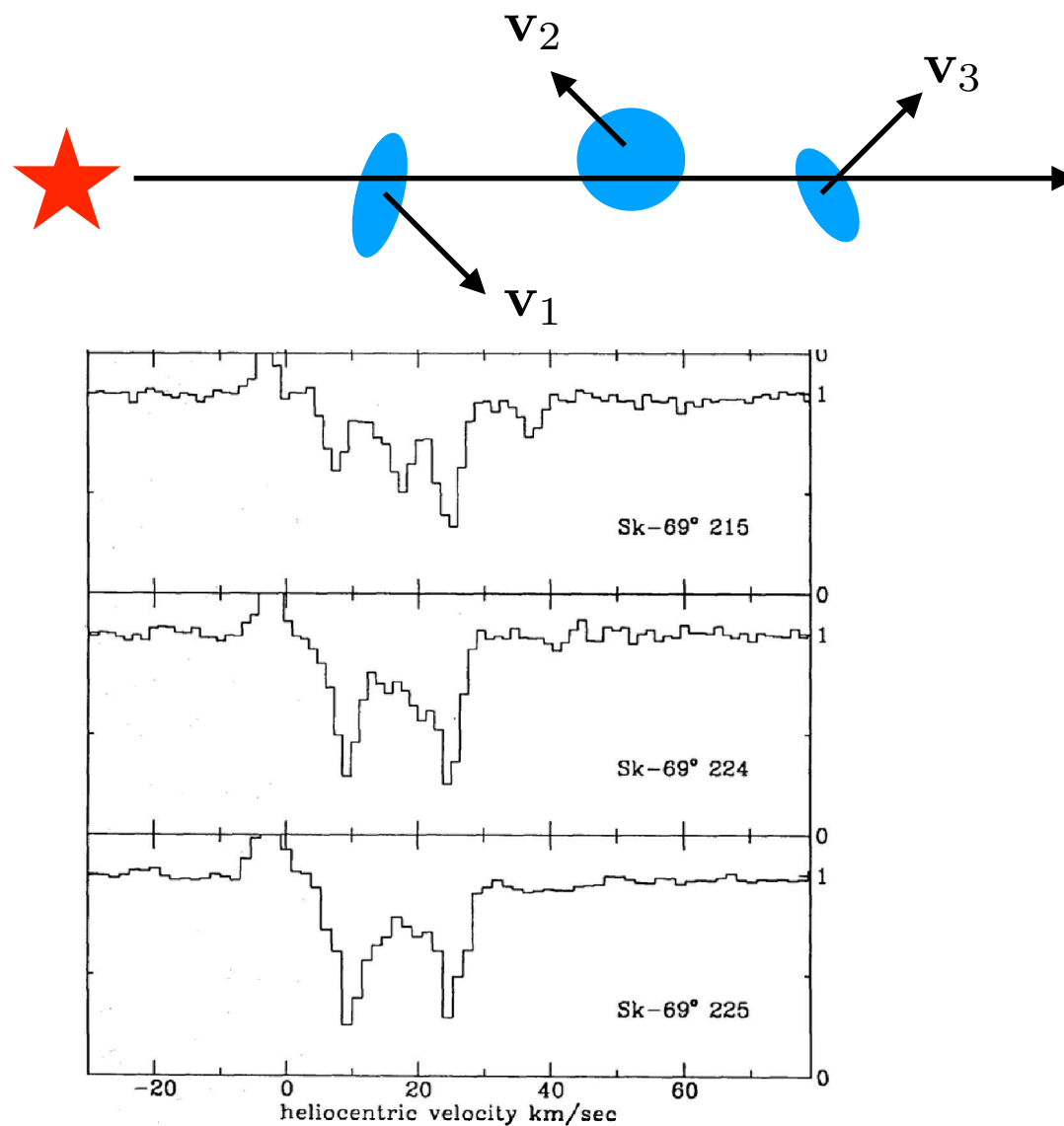
Overall Properties of the Cold Neutral Medium (CNM)

- Overall properties of the CNM
 - Temperature $T \sim 100 \text{ K}$
 - Mean kinetic energy per particle $\langle E \rangle = (3/2)kT \sim 0.013 \text{ eV}$
 - Number density
 - ▶ $n_{\text{atom}} \sim 30 \text{ cm}^{-3}$ for atoms
 - ▶ $n_e \sim 0.04 \text{ cm}^{-3}$ for free electrons
 - Thermal velocity
 - ▶ $v_{\text{th}}(\text{H}) \sim 1.6 \text{ km s}^{-1}$ for hydrogen atoms
 - ▶ $v_{\text{th}}(e) \sim 67 \text{ km s}^{-1}$ for free electrons
 - Mean free path
 - ▶ $\lambda_{\text{mfp}}(\text{HH}) \sim 0.74 \text{ AU}$ for atom-atom collisions
 - ▶ $\lambda_{\text{mfp}}(e\text{H}) \sim 1700 \text{ AU}$ for atom-electron collisions
 - ▶ $\lambda_{\text{mfp}}(ee) \sim 1.9 \times 10^{-3} \text{ AU}$ for electron-electron collisions
 - Collisional time scale
 - ▶ $t_{\text{coll}}(\text{HH}) \sim 2.2 \text{ yr}$ for atom-atom collisions
 - ▶ $t_{\text{coll}}(e\text{H}) \sim 120 \text{ yr}$ for atom-electron collisions
 - ▶ $t_{\text{coll}}(ee) \sim 1.2 \text{ hr}$ for electron-electron collision

See [reference - collisional time scale.pdf](#)
for the detailed calculations of the numerical values

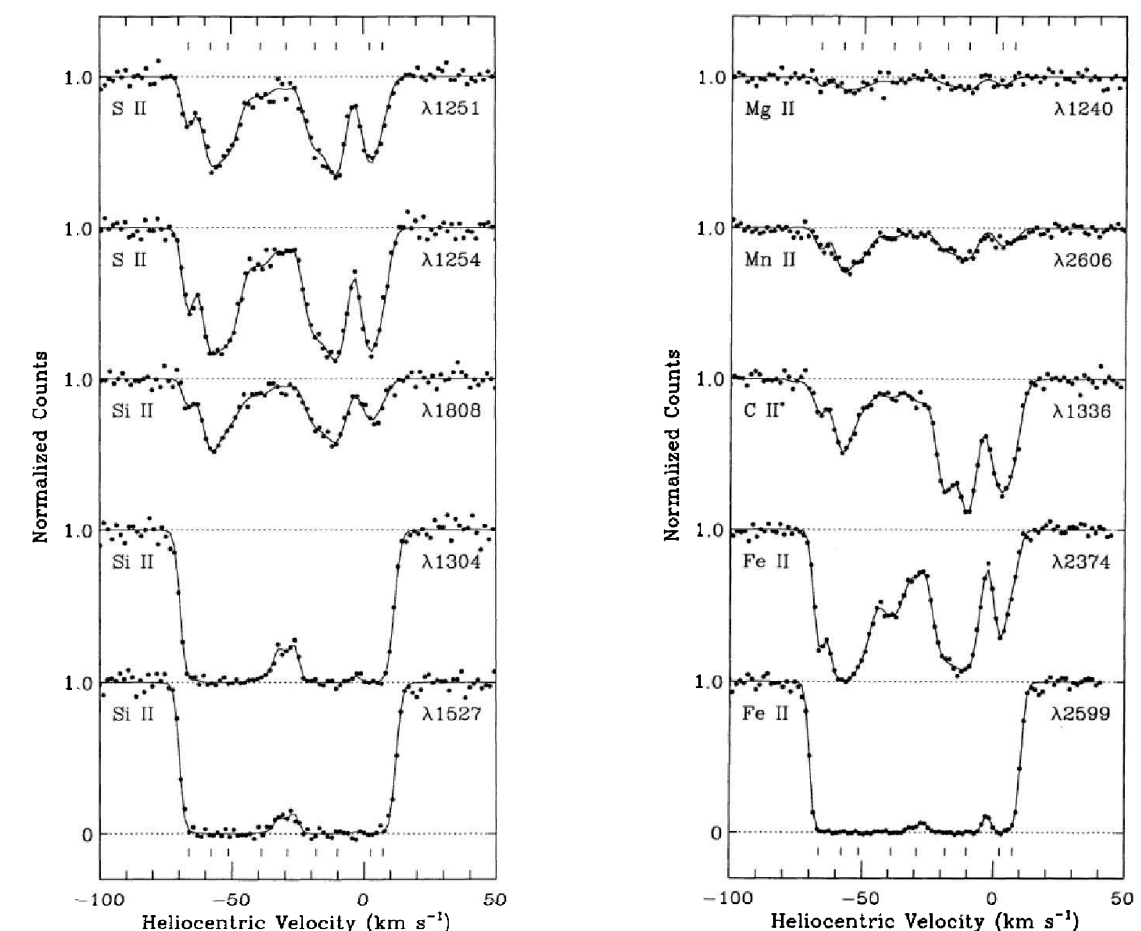
Observations of Absorption Lines Toward the CNM

- The CNM gives rise to a number of absorption features in the spectra of hot background stars (and quasars).
 - The most prominent absorption lines at visible wavelengths are Ca II K and H lines at $\lambda = 3933, 3968 \text{ \AA}$, and Na I D₁ and D₂ doublet lines at $\lambda = 5890, 5896 \text{ \AA}$.



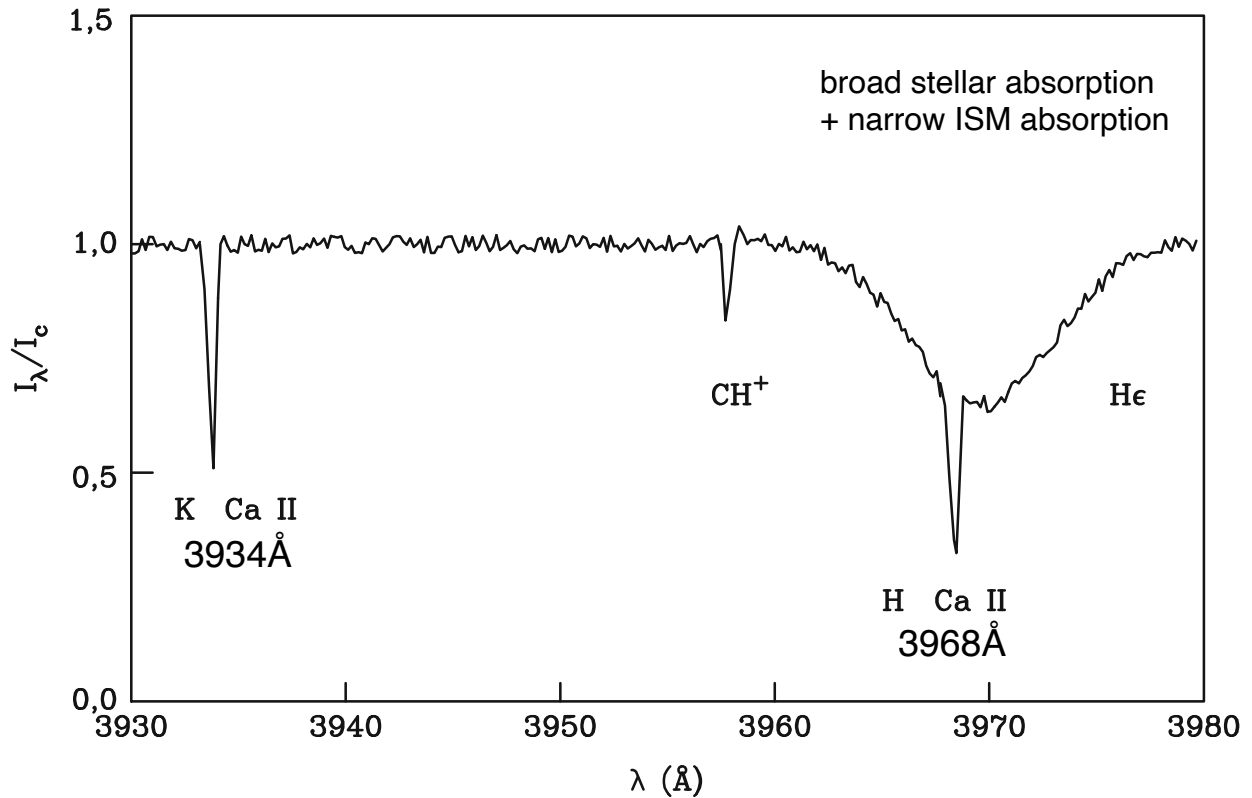
Na I D₂ interstellar absorption line seen along 3 lines of sight to stars in LMC (Molaro et al. 1993)

[Note] The cold gas is ~ 100 pc away from Earth, meaning that 5 arcmin corresponds to ~ 0.15 pc.



UV interstellar absorption lines toward an O-type star HD93521. (Spitzer & Fitzpatrick 1993)

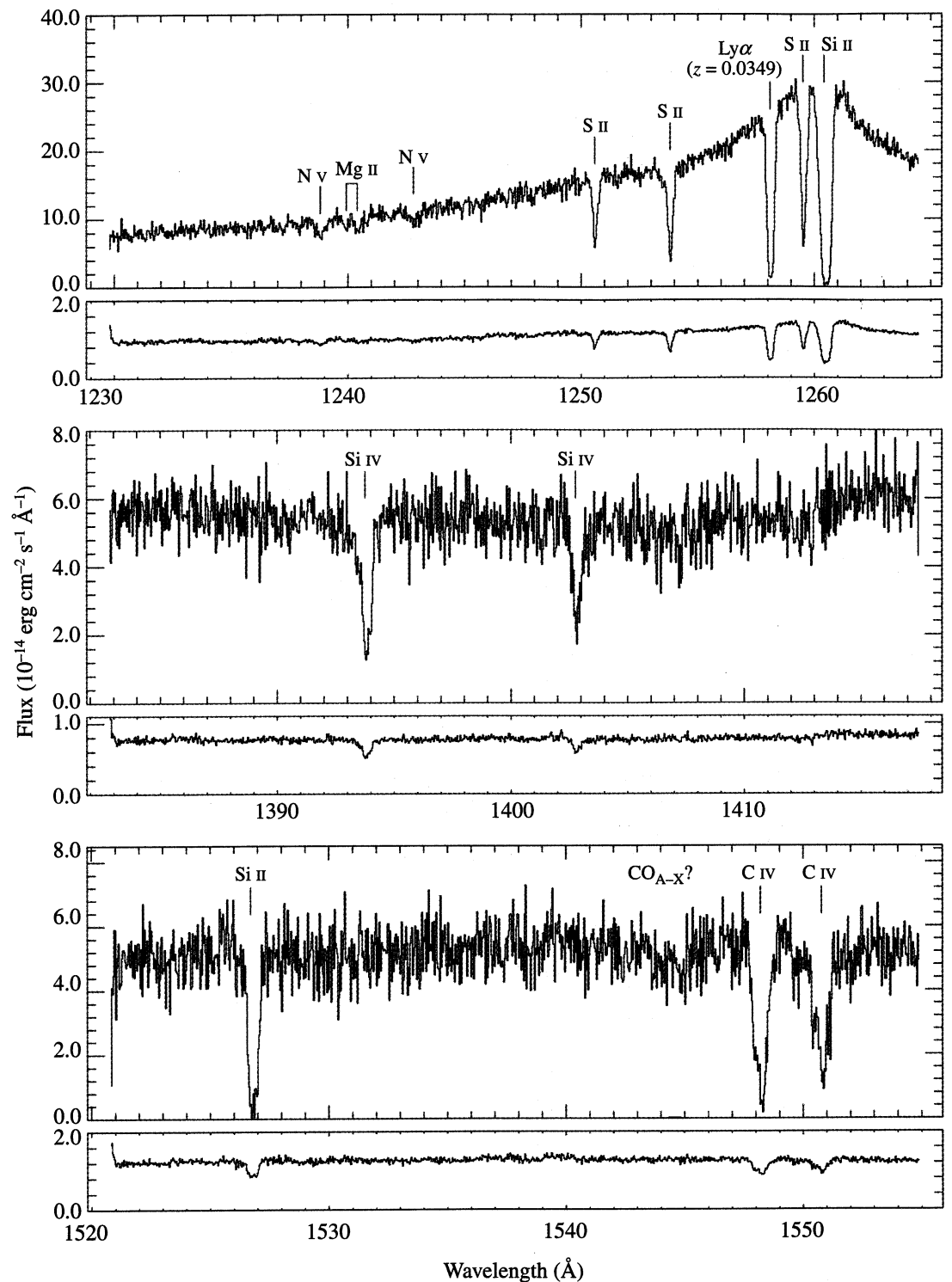
[Note] (1) multiple velocity components and (2) line saturation on Si II and Fe II.
The multiple velocities are due primarily to the differential rotation of our galaxy. (clouds at different distances)



Interstellar absorption lines in the spectrum of ζ Oph (O9.5V).

Note that the Ca II H line occurs inside the He hydrogen line, which is much broader and of stellar origin.

Figure 4.6 in Astrophysics of the Interstellar Medium [Maciel]



Interstellar absorption lines toward the Seyfert 1 galaxy ESO 141-055.

Figure 5.5 in Physics and Chemistry of the Interstellar Medium [Kwok]

- The alkali metals (Li, K, and Na) and alkaline earth metals (Ca) produce absorption lines at visible wavelengths ($4000 \text{ \AA} < \lambda < 7300 \text{ \AA}$, $1.7 \text{ eV} < E < 3.1 \text{ eV}$); these elements have loosely bound outer electrons.
- Most other elements produce UV absorption lines ($\lambda < 4000 \text{ \AA}$, $E > 3.1 \text{ eV}$).
 - Therefore, the study of the CNM was extensively made by the launch of orbiting UV telescopes (Copernicus, IUE, etc).
 - In particular, Ly α ($\lambda = 1215.67 \text{ \AA}$; $E = 10.2 \text{ eV}$) from hydrogen.
- Interstellar absorption lines at visible wavelengths were also found from neutral atoms such as Ca I, K I, Li I, ions such as Ti II, and diatomic molecules such as CH, NH, CN, CH⁺ and C₂.
 - [Note] The first discovery of interstellar molecules was made by the detection of CH absorption at $\lambda \sim 4300$ (4315) \AA (Swings & Rosenfeld 1937, ApJ), not at radio wavelengths.
 - CH, NH, and CN are referred to as “**radicals**”, in chemistry, meaning molecules that contain at least one unpaired electron. They quickly combine with one another, or with single atoms in laboratory. But, in the low density of the ISM, they have long lifetimes.

- The composition and excitation of interstellar gas can be studied using absorption lines that appear in the spectra of background stars (or other sources).
- The interstellar lines are typically narrow compared to spectral features produced by absorption in stellar photospheres, and in practice can be readily distinguished.
 - For instance, consider the Fraunhofer lines in the Sun's spectrum. The Ca H and K lines, with equivalent widths of 14Å and 19Å respectively, are the strongest absorption lines. The Na I D₁ and D₂ lines have equivalent widths of 0.6Å and 0.8Å.
 - On the other hand, for many interstellar lines, the equivalent width is sufficiently small that the mÅ is a convenient unit.
- It is normally possible to detect absorption only by the ground state (and perhaps the excited fine-structure levels of the ground electronic state) - the populations in the excited electronic states are too small to be detected in absorption.
- The widths of absorption lines are usually determined by Doppler broadening, with line widths of a few km s⁻¹ (or $\Delta\lambda/\lambda \approx 10^{-5}$) - often observed in cool clouds.
- Absorption lines (and emission lines) contains a lots of information about number density, temperature, chemical abundances, ionization states, and excitation states.
- However, interpreting the information requires understanding the ways in which light interacts with baryonic matter, radiative transfer.
- **We need to know the line profile to analyze absorption lines.**

Optical Depth

- The optical depth in an absorption line can be written

$$\tau_\nu = \frac{\pi e^2}{m_e c} f_{\ell u} \left(1 - \frac{n_u/g_u}{n_\ell/g_\ell} \right) N_\ell \phi_\nu \simeq \frac{\pi e^2}{m_e c} f_{\ell u} N_\ell \phi_\nu$$

Here, $N_\ell \equiv \int n_\ell ds$ is the column density of the absorbers.

The line profile is given by $\phi_\nu = \frac{1}{\Delta\nu_D \sqrt{\pi}} H(u, a)$, and its value at the line center is

$$\begin{aligned} \phi_\nu(\nu = \nu_{\ell u}) &= \frac{1}{\nu_{\ell u}(b/c)\sqrt{\pi}} H(0, a) & u &= \frac{\nu - \nu_{\ell u}}{\Delta\nu_D} = \frac{\nu - \nu_{u\ell}}{\nu_{\ell u}(b/c)} \\ &\approx \frac{1}{\nu_{\ell u}(b/c)\sqrt{\pi}} & &= \frac{v}{b} \quad \left(v = \frac{\nu - \nu_{\ell u}}{\nu_{\ell u}} c, \quad b = \sqrt{2}v_{\text{rms}} = \sqrt{\frac{2k_B T}{m}} \right) \end{aligned}$$

The correction factor for stimulated emission is negligible for the optical lines. Then, dropping the correction factor, the optical depth can be written

$$\tau_\nu = \tau_0 H(u, a) \quad \text{Here, } \tau_0 \text{ is the optical depth at the line center.}$$

$$\tau_0 = \frac{\pi e^2}{m_e c} f_{\ell u} \frac{1}{\nu_{\ell u}(b/c)\sqrt{\pi}} N_\ell = \frac{\sqrt{\pi} e^2}{m_e c} f_{\ell u} \frac{\lambda_{\ell u}}{b} N_\ell$$

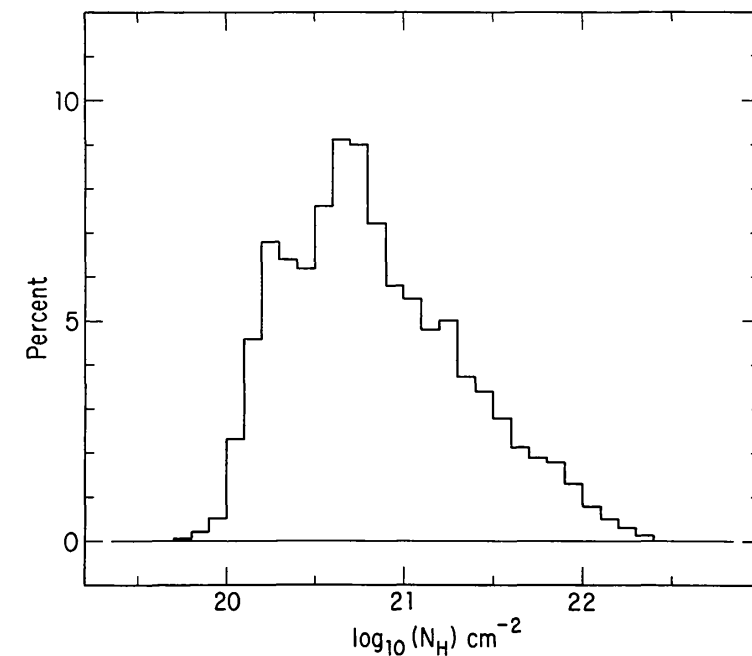
- The central optical depth for Ly α is

$$\tau_0 = 0.7580 \left(\frac{N_\ell}{10^{13} \text{ cm}^{-2}} \right) \left(\frac{f_{\ell u}}{0.4164} \right) \left(\frac{\lambda_{\ell u}}{1215.67 \text{ \AA}} \right) \left(\frac{10 \text{ km s}^{-1}}{b} \right)$$

- In the WNM ($b \approx 10 \text{ km s}^{-1}$), Ly α will be optically thin ($\tau_0 < 1$) when $N_\ell < 10^{13} \text{ cm}^{-2}$ and optically thick ($\tau_0 > 1$) when $N_\ell > 10^{13} \text{ cm}^{-2}$.
- In the CNM ($b \approx 1 \text{ km s}^{-1}$), Ly α will be optically thin when $N_\ell < 10^{12} \text{ cm}^{-2}$ and optically thick when $N_\ell > 10^{12} \text{ cm}^{-2}$.
- In Milky Way, the total column density of hydrogen atom is $N_\ell \sim 10^{20} - 10^{22} \text{ cm}^{-2}$.

The percentage of the sky covered by H I at a given N_H .

Figure 4 in [Dickey & Lockman \(1990, ARA&A\)](#)



- As a reference, the column density of the Earth's atmosphere, looking upward from sea level, is $N \sim 2 \times 10^{25} \text{ cm}^{-2}$.

Absorption Line Shapes

- Lyman α absorption line profiles for $b = 10 \text{ km s}^{-1}$

$$F_\nu/F_\nu(0) = e^{-\tau_0 H(u,a)}$$

- When $\tau_0 < 1$, $F_\nu/F_\nu(0) \approx 1 - \tau_\nu$ and thus the shape of an absorption line resembles the upside-down Voight function.
- When $\tau_0 \gg 1$, the absorption line saturates at its center and becomes increasingly “box-shaped.”

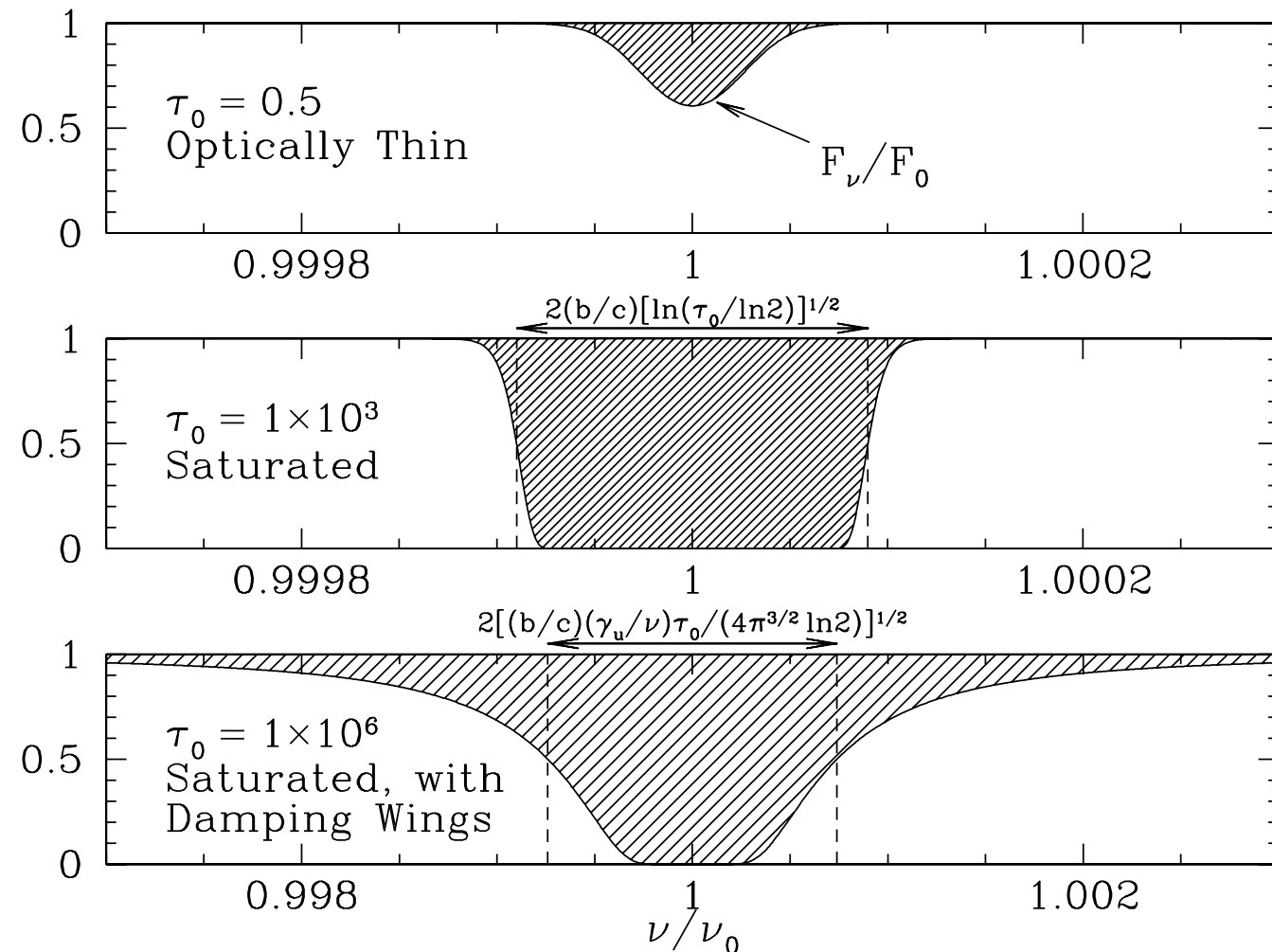
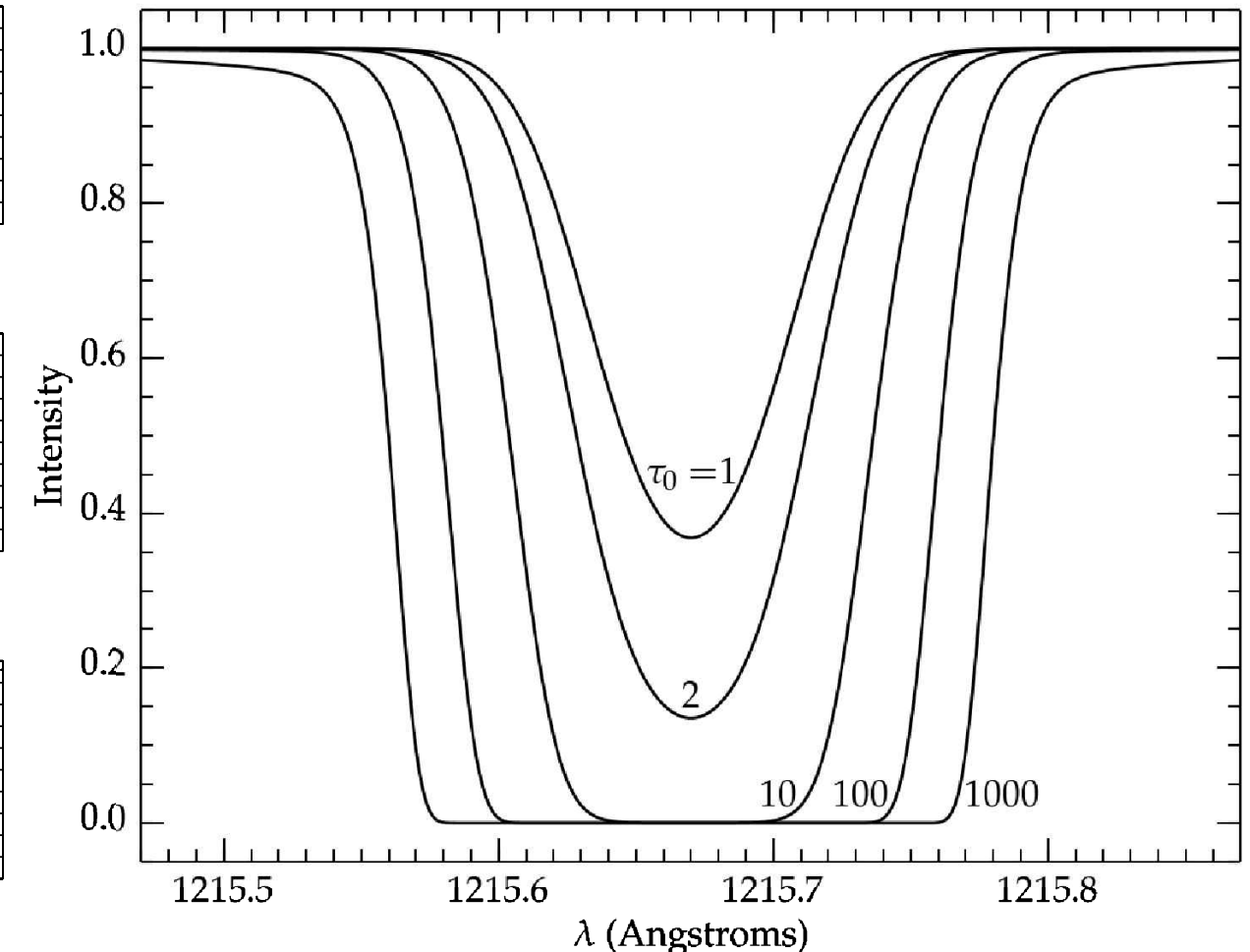


Figure 9.1 in [Draine]

Note the different abscissa in the lowest panel.



Lyman α absorption lines for $b = 10 \text{ km s}^{-1}$.

Figure 2.6 in [Ryden]

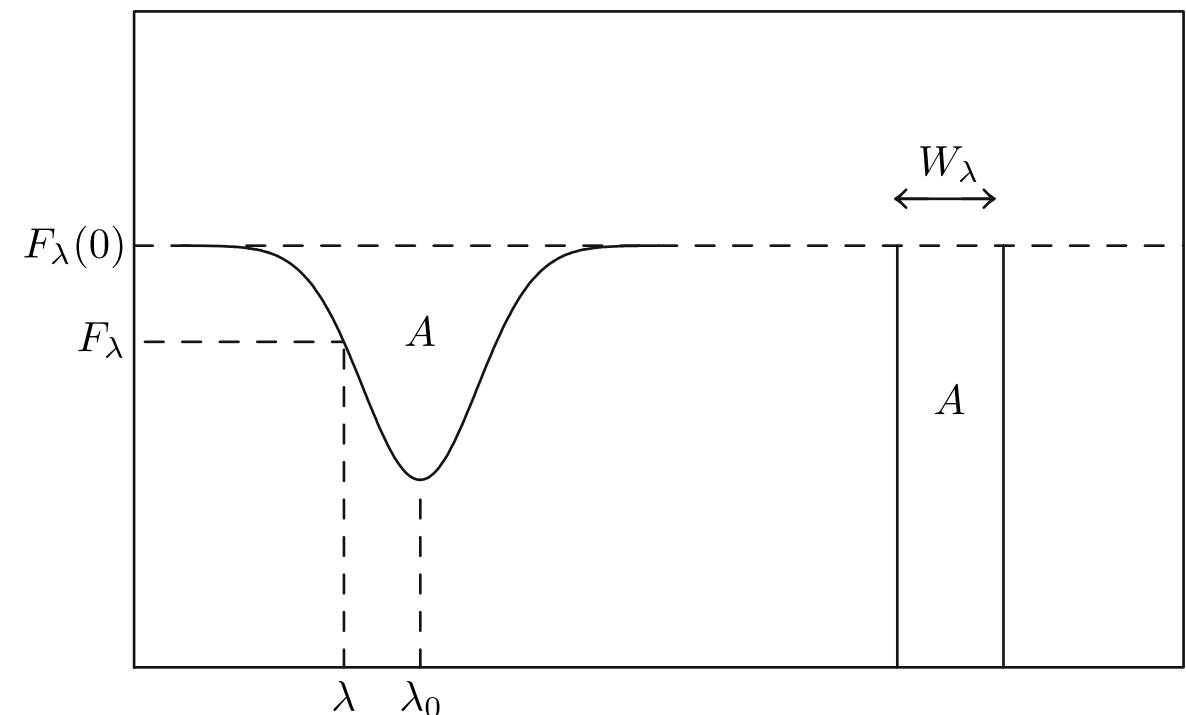
Equivalent Width & Curve of growth

- ***Equivalent width***

- The spectrograph often lacks the spectral resolution to resolve the profiles of narrow lines, but can measure the total amount of “missing power” resulting from a narrow absorption line.
- *The equivalent width is a measure of the strength of an absorption line, in terms of “missing power” in the unresolved absorption line.*

A diagram illustrating the absorption of radiation. A blue rectangle represents the initial flux density at zero separation, labeled $F_\nu(0)$. An arrow points from this to a smaller rectangle labeled $F_\nu(s)$, representing the flux density after passing through a medium. Below the diagram is the equation:

$$F_\nu = F_\nu(0)e^{-\tau_\nu}$$



- ***Curve of growth***

- The curve of growth refers to the numerical relation between the observed equivalent width and the underlying optical depth (or the column density) of the absorber.

Equivalent Width

- Suppose that we measure the energy flux density F_ν using an aperture of solid angle $\Delta\Omega$. Then, we obtain the flux density at the observer:

$$F_\nu = F_\nu(0)e^{-\tau_\nu} + B_\nu(T_{\text{exc}})\Delta\Omega(1 - e^{-\tau_\nu})$$

Here, $F_\nu(0)$ is the flux density of the background light source.

- At optical frequencies and in the neutral medium, nearly all atoms are in their ground state. Thus, we normally have $n_u/n_\ell \ll 1$ and $B_\nu(T_{\text{exc}})\Delta\Omega \ll F_\nu(0)$. Then, we can neglect the emission from the ISM.

$$F_\nu = F_\nu(0)e^{-\tau_\nu}$$



$$\frac{h\nu}{k_B T_{\text{exc}}} = \frac{6000 \text{ \AA}}{\lambda} \frac{2.4 \times 10^4 \text{ K}}{T_{\text{exc}}}$$

- If the background spectrum is smooth, we can define the **dimensionless equivalent width** and the **wavelength equivalent width** as follows:

$$W \equiv \int \frac{d\nu}{\nu_0} \left[1 - \frac{F_\nu}{F_\nu(0)} \right] = \int \frac{d\nu}{\nu_0} (1 - e^{-\tau_\nu})$$

$$W_\lambda \equiv \int d\lambda (1 - e^{-\tau_\lambda}) \approx \lambda_0 W$$

- The equivalent width is the width of a straight-sided, perfectly black absorption line that has the same integrated flux deficit as the actual absorption line.

Overall Shape of the Curve of Growth

The Curve of Growth

= the relation between optical depth at line center and equivalent width

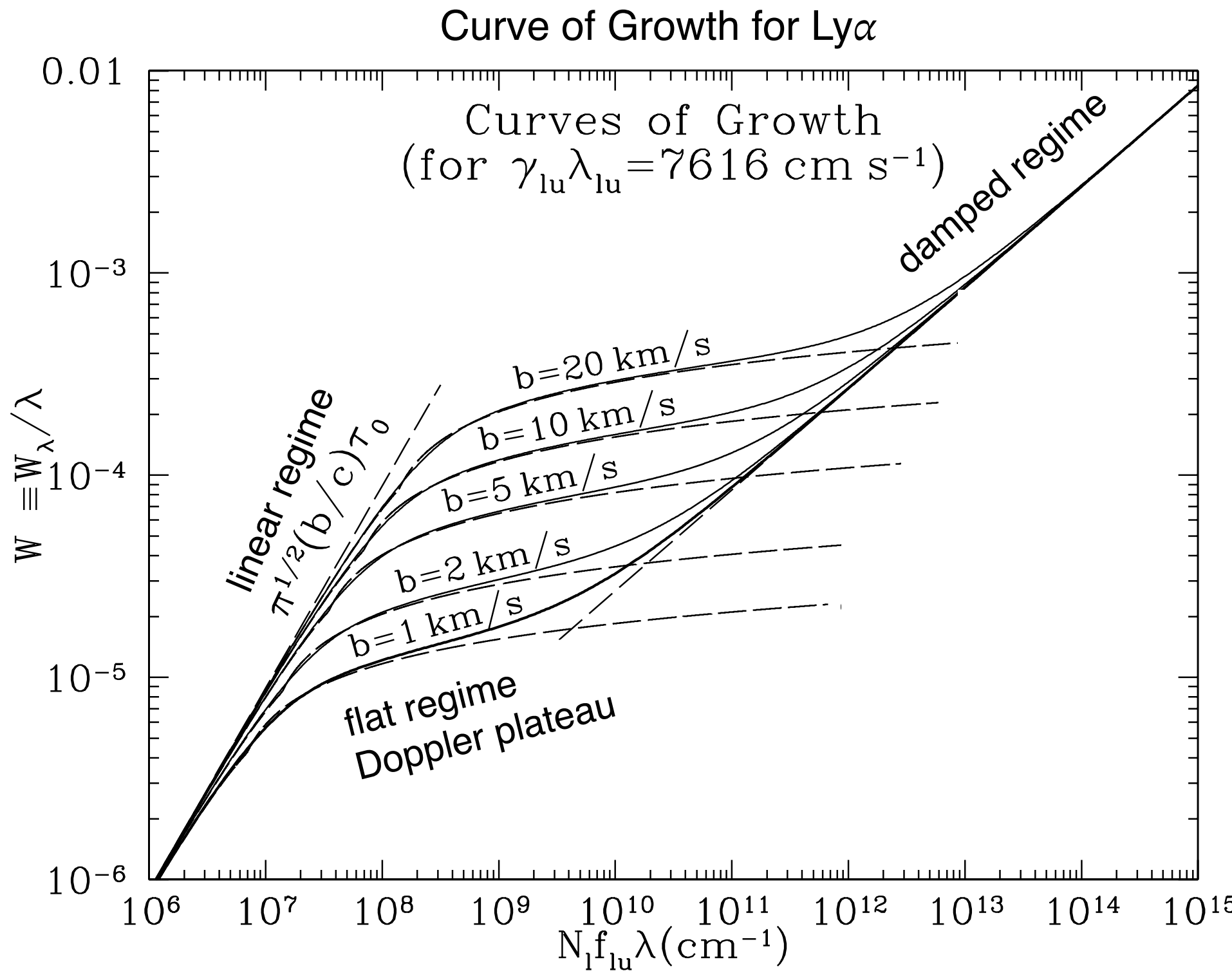


Figure 9.2 in [Draine]

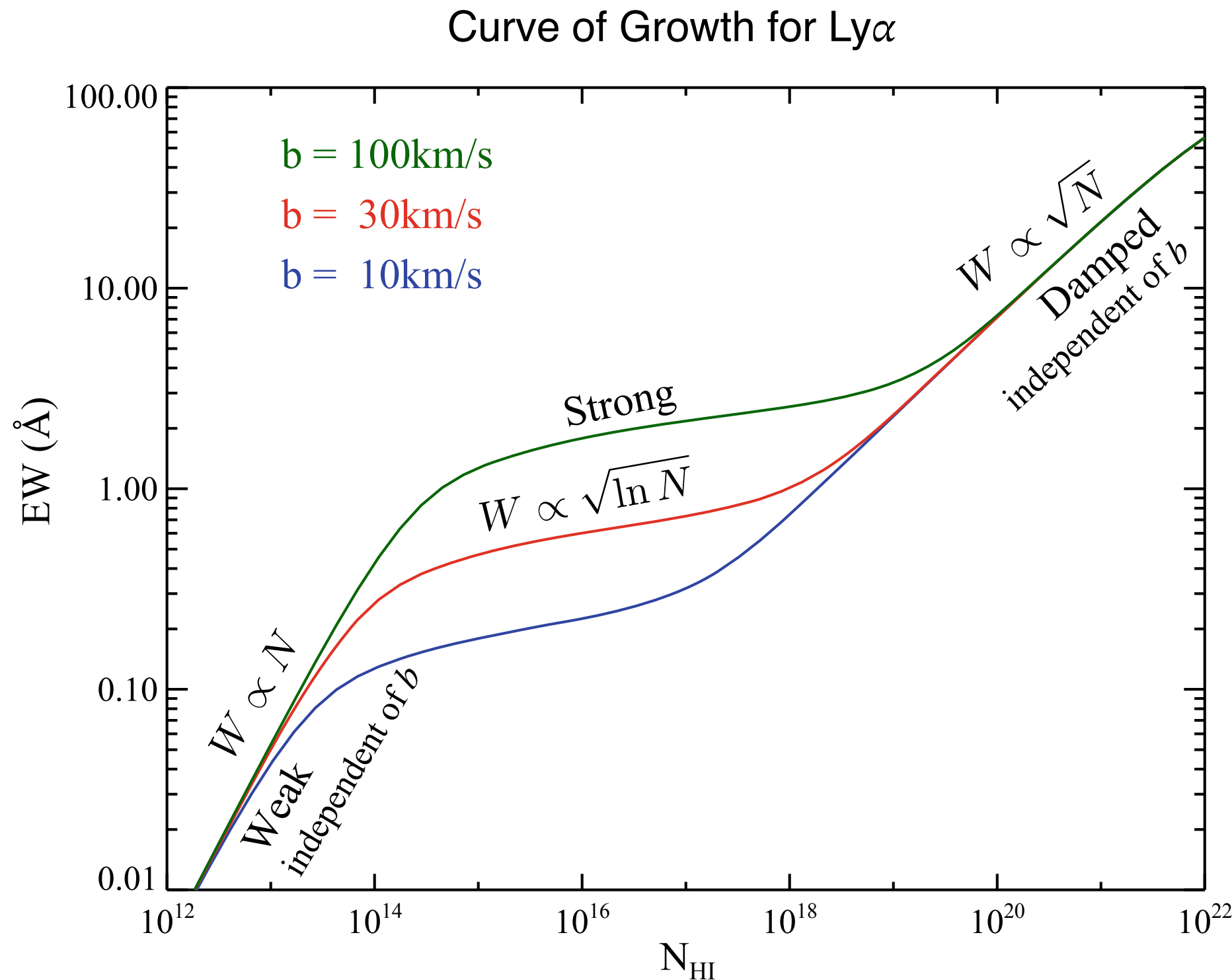


Figure 2.10 in Chap. 2 [Prochaska]
Lyman-alpha as An Astrophysical and Cosmological Tool

Detailed Analysis of The Curve of Growth

- **Equivalent width:**

$$W = \int_{-\infty}^{\infty} \frac{d\nu}{\nu_0} (1 - e^{-\tau_\nu}) = \frac{b}{c} \int_{-\infty}^{\infty} du (1 - e^{-\tau_\nu})$$

- ***Optically Thin Absorption, $\tau_0 \lesssim 1$ (linear regime)***

$$\begin{aligned} W &= \frac{b}{c} \int_{-\infty}^{\infty} du \left(\tau_\nu - \frac{\tau_\nu^2}{2} + \dots \right) \approx \frac{b}{c} \int_{-\infty}^{\infty} du \left(\tau_0 e^{-u^2} - \tau_0^2 \frac{e^{-2u^2}}{2} + \dots \right) \\ &= \sqrt{\pi} \frac{b}{c} \tau_0 \left(1 - \frac{\tau_0}{2\sqrt{2}} + \dots \right) \end{aligned}$$

↑
 $\tau_\nu = \tau_0 H(u, a) \approx \tau_0 e^{-u^2}$ if $a \ll 1$

$$\begin{aligned} W &\approx \sqrt{\pi} \frac{b}{c} \frac{\tau_0}{1 + \tau_0/(2\sqrt{2})} && \xleftarrow{\hspace{1cm}} 1 - x \approx \frac{1}{1 + x} \\ &= \frac{\pi e^2}{m_e c^2} N_\ell f_{\ell u} \lambda_{\ell u} \frac{1}{1 + \tau_0/(2\sqrt{2})} && \xleftarrow{\hspace{1cm}} \tau_0 = \frac{\sqrt{\pi} e^2}{m_e c} f_{\ell u} \frac{\lambda_{\ell u}}{b} N_\ell \end{aligned}$$

$$\begin{aligned} W &= 4.48 \times 10^{-6} \left(\frac{N_\ell}{10^{12} \text{ cm}^{-2}} \right) \left(\frac{f_{\ell u}}{0.4164} \right) \left(\frac{\lambda_{\ell u}}{1215.67 \text{ \AA}} \right) \\ N_\ell &= 1.84 \times 10^{12} \text{ cm}^{-2} \left(\frac{0.4164}{f_{\ell u}} \right) \left(\frac{1215.67 \text{ \AA}}{\lambda_{\ell u}} \right)^2 \left(\frac{W_\lambda}{0.01 \text{ \AA}} \right) \text{ if } \tau_0 \lesssim 1 \end{aligned}$$

← $N_\ell = W \frac{m_e c^2}{\pi e^2} \frac{1}{f_{\ell u} \lambda_{\ell u}}$
 $W \approx \frac{W_\lambda}{\lambda_{\ell u}}$

The measurement of W allows us to determine N_ℓ , provided that the line is optical thin.

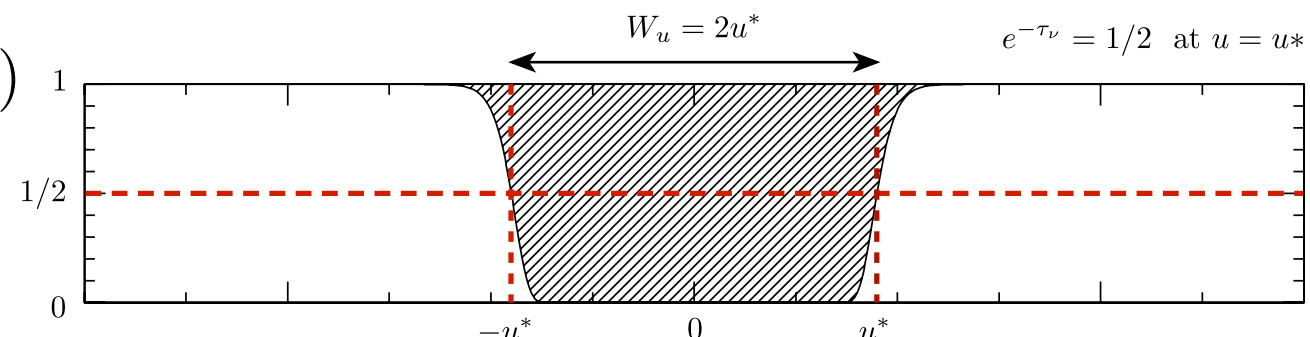
- **Flat Portion of the Curve of Growth, $1 < \tau_0 \lesssim \tau_{\text{damp}}$**

- Now consider what happens when an absorption line is optically thick, but not so optically thick that the broad Lorentz wing ν^{-2} provides a significant contribution to the absorption.
- The optical depth at which the wing becomes important is called the ***damping optical depth*** τ_{damp} .

$$W = \frac{b}{c} \int_{-\infty}^{\infty} du \left[1 - \exp \left(-\tau_0 e^{-u^2} \right) \right]$$

- The absorption line shape is almost “box-shaped.” We assume that the term in square brackets equals “1” until a certain value u_* and then, suddenly drops to “0”.
- We define u_* to be the location at half maximum of the square brackets:

$$\exp \left(-\tau_0 e^{-u_*^2} \right) = \frac{1}{2} \rightarrow u_*^2 = \ln (\tau_0 / \ln 2)$$



- Then, we have

$$W \approx \frac{b}{c} \int_{-u_*}^{u_*} du = \frac{b}{c} (2u_*) \longrightarrow W \approx \frac{2b}{c} \sqrt{\ln (\tau_0 / \ln 2)}$$

- Note that W is very insensitive to τ_0 (and thus N_ℓ) in this regime. Because W increases so slowly with increasing N_ℓ , this is referred to as the flat portion of the curve of growth.

-
- Inverting the above equation, we obtain

$$\tau_0 \approx (\ln 2) \exp \left[\left(\frac{cW}{2b} \right)^2 \right]$$

$$N_\ell \approx \frac{\ln 2}{\sqrt{\pi}} \frac{m_e c}{e^2} \frac{b}{f_{\ell u} \lambda_{\ell u}} \exp \left[\left(\frac{cW}{2b} \right)^2 \right]$$

$$N_\ell \approx 9.15 \times 10^{12} \text{ cm}^{-2} \left(\frac{0.4164}{f_{\ell u}} \right) \left(\frac{1215.67 \text{ \AA}}{\lambda_{\ell u}} \right) \left(\frac{b}{10 \text{ km s}^{-1}} \right)$$

$$\times \exp \left[0.0152 \left(\frac{1215.67 \text{ \AA}}{\lambda_{\ell u}} \right)^2 \left(\frac{10 \text{ km s}^{-1}}{b} \right)^2 \left(\frac{W_\lambda}{0.01 \text{ \AA}} \right)^2 \right]$$

- ***The column density at a given equivalent width depends on the temperature***, and thus on the thermal broadening.
- Any error in evaluating W_λ (from misestimating the continuum flux, for instance) will propagate exponentially into an error in N_ℓ .
- Therefore, it is advised not to use the above equation unless you have a very good idea of what the equivalent width W_λ and the thermal broadening b are for the sightline in question.

- **Damped Portion of the Curve of Growth, $\tau_0 \gtrsim \tau_{\text{damp}}$ (square-root regime)**

- In this regime, the Doppler core of the line is totally saturated, but the “damping wing” of the Voigt profile start to contribute significantly to the equivalent width.

$$W = \frac{b}{c} \int_{-\infty}^{\infty} du \left[1 - \exp \left(-\tau_0 \frac{a}{\sqrt{\pi} u^2} \right) \right]$$

$$\begin{aligned} \exp(-\tau_0 e^{-u^2}) &= 0 && \text{if } \tau_0 \gtrsim \tau_{\text{damp}} \text{ and } u \lesssim u_* \\ \exp\left(-\tau_0 \frac{a}{\sqrt{\pi} u^2}\right) &= 0 \end{aligned}$$

change of variables: Let $\tau_0 \frac{a}{\sqrt{\pi} u^2} = \frac{1}{x^2} \rightarrow u = \left(\frac{\tau_0 a}{\sqrt{\pi}}\right)^{1/2} x$

$$W = \frac{b}{c} \left(\frac{\tau_0 a}{\sqrt{\pi}}\right)^{1/2} \int_{-\infty}^{\infty} dx \left[1 - \exp(-1/x^2) \right] = \frac{b}{c} \left(\frac{\tau_0 a}{\sqrt{\pi}}\right)^{1/2} 2\sqrt{\pi}$$

Therefore, we have

$$W = \frac{b}{c} (4\sqrt{\pi} \tau_0 a)^{1/2}$$

$$a = \frac{\gamma_{\ell u}}{4\pi} \frac{1}{\nu_{\ell u}(b/c)} = \frac{\gamma_{\ell u}}{4\pi} \frac{\lambda_{\ell u}}{b}$$

$$W = \sqrt{\frac{b}{c} \frac{\tau_0}{\sqrt{\pi}} \frac{\gamma_{\ell u} \lambda_{\ell u}}{c}} \rightarrow \tau_0 = \sqrt{\pi} \frac{c}{b} \frac{c}{\gamma_{\ell u} \lambda_{\ell u}} W^2$$

$$\begin{aligned} I &\equiv \int_{-\infty}^{\infty} dx \left(1 - e^{-1/x^2} \right) = 2 \int_0^{\infty} dx \left(1 - e^{-1/x^2} \right) \\ &= 2 \int_0^{\infty} \frac{dy}{y^2} \left(1 - e^{-y^2} \right) \quad \leftarrow y = 1/x \\ &= 2 \left[-\frac{1}{y} \left(1 - e^{-y^2} \right) \right]_0^{\infty} + 2 \int_0^{\infty} \frac{1}{y} \left(2ye^{-y^2} \right) dy \\ &= \lim_{y \rightarrow 0} \frac{2}{y} \left(1 - e^{-y^2} \right) + 4 \int_0^{\infty} e^{-y^2} dy \\ &= \lim_{y \rightarrow 0} \frac{2}{y} (1 - 1 + y^2) + 2 \int_{-\infty}^{\infty} e^{-y^2} dy = 2\sqrt{\pi} \end{aligned}$$

-
- Approximation of the absorption profile as a boxy shape (square brackets)
 - B. T. Draine (2011) defines u_* to be the location at half maximum (FWHM = $2u^*$), and calculates the EW.

$$\exp\left(-\tau_0 \frac{a}{\sqrt{\pi} u_*^2}\right) = \frac{1}{2} \longrightarrow u_*^2 = \frac{\tau_0}{\sqrt{\pi}} \frac{a}{\ln 2}$$

$$W \approx \frac{b}{c} \int_{-u_*}^{u_*} du = \frac{b}{c} (2u_*) \longrightarrow W \approx \frac{2b}{c} \sqrt{\frac{\tau_0}{\sqrt{\pi}} \frac{a}{\ln 2}}$$

$a = \frac{\gamma_{\ell u}}{4\pi} \frac{1}{\nu_{\ell u}(b/c)} = \frac{\gamma_{\ell u}}{4\pi} \frac{\lambda_{\ell u}}{b}$

$$= \frac{1}{\sqrt{\pi \ln 2}} \sqrt{\frac{b}{c} \frac{\tau_0}{\sqrt{\pi}} \frac{\gamma_{\ell u} \lambda_{\ell u}}{c}}$$

He note that this value is smaller than by a factor of $\sqrt{\pi \ln 2} = 1.476$. Multiplying by this factor, he obtain the same result as ours.

- Our result is the same as that obtained using the following u_* :

$$\exp\left(-\tau_0 \frac{a}{\sqrt{\pi} u_*^2}\right) = \exp\left(-\frac{1}{\pi}\right) = 0.7274$$

$$u_*^2 = \frac{\tau_0}{\sqrt{\pi}} (\pi a) = \pi \ln 2 \left(\frac{\tau_0}{\sqrt{\pi}} \frac{a}{\ln 2} \right) \longrightarrow W = \frac{b}{c} (2u_*) = \frac{b}{c} (4\sqrt{\pi \tau_0 a})^{1/2}$$

$$N_\ell = \frac{m_e c^3}{e^2} \frac{1}{f_{\ell u} \gamma_{\ell u} \lambda_{\ell u}^2} W^2 = \frac{m_e c^3}{e^2} \frac{1}{f_{\ell u} \gamma_{\ell u} \lambda_{\ell u}^4} W_\lambda^2$$

$$N_\ell = 1.867 \times 10^{18} \text{ cm}^{-2} \left(\frac{0.4164}{f_{\ell u}} \right) \left(\frac{6.265 \times 10^8 \text{ s}^{-1}}{\gamma_{\ell u}} \right) \left(\frac{1215.67 \text{ \AA}}{\lambda_{\ell u}} \right)^4 \left(\frac{W_\lambda}{1 \text{ \AA}} \right)^2$$

- The equivalent width is proportional to the square-root of the optical depth. The column density (optical depth) is proportional to the square of the measured equivalent width.
- Furthermore, ***the column density is independent of the thermal broadening.***
- The ***damping optical depth*** at which the transition from the flat to the damped portion of the curve of growth occurs are obtained by setting $W^{\text{flat}} = W^{\text{sq.-root}}$.

$$\frac{2b}{c} \sqrt{\ln(\tau_{\text{damp}} / \ln 2)} = \sqrt{\frac{b}{c} \frac{\tau_{\text{damp}}}{\sqrt{\pi}} \frac{\gamma_{\ell u} \lambda_{\ell u}}{c}}$$

\Rightarrow

$$\tau_{\text{damp}} = 4\sqrt{\pi} \frac{b}{\gamma_{\ell u} \lambda_{\ell u}} \ln(\tau_{\text{damp}} / \ln 2)$$

$$\approx 4\sqrt{\pi} \frac{b}{\gamma_{\ell u} \lambda_{\ell u}} \ln \left(\frac{4\sqrt{\pi}}{\ln 2} \frac{b}{\gamma_{\ell u} \lambda_{\ell u}} \right)$$

An approximate solution for (when $q \gg 1$)

$$y = q \ln(y / \ln 2) \rightarrow \text{set } x = y / \ln 2 \text{ and } C = q / \ln 2 \\ \rightarrow x = C \ln(x)$$

We use the fixed point iteration method.

$$\begin{aligned} x^{(0)} &= e & x^{(3)} &= C \ln x^{(2)} \\ x^{(1)} &= C \ln x^{(0)} = C & &= C \ln C + C \ln(\ln C) \\ x^{(2)} &= C \ln x^{(1)} = C \ln C \end{aligned}$$

Then, we obtain an approximate solution:

$$x \approx x^{(2)} = C \ln C \rightarrow y \approx q \ln(q / \ln 2)$$

This solution is found to underestimate τ_{damp} by a factor of ~ 1.4 (~ 1.3) for $b = 1$ (10) km s^{-1} .

$$C \equiv 4\sqrt{\pi} \frac{b}{\gamma_{\ell u} \lambda_{\ell u}} = 93.1 \left(\frac{b}{1 \text{ km s}^{-1}} \right) \left(\frac{6.265 \times 10^8 \text{ s}^{-1}}{\gamma_{\ell u}} \right) \left(\frac{1215.67 \text{ \AA}}{\lambda_{\ell u}} \right)$$

$$\begin{aligned} \tau_{\text{damp}} &\approx 93.1 \left(\frac{b}{1 \text{ km s}^{-1}} \right) \left(\frac{7616 \text{ cm s}^{-1}}{\gamma_{\ell u} \lambda_{\ell u}} \right) \ln \left[134 \left(\frac{b}{1 \text{ km s}^{-1}} \right) \left(\frac{7616 \text{ cm s}^{-1}}{\gamma_{\ell u} \lambda_{\ell u}} \right) \right] \\ &= 456 \left(\frac{b}{1 \text{ km s}^{-1}} \right) \left[1 + 0.204 \ln \left(\frac{b}{1 \text{ km s}^{-1}} \right) \right] \\ &= 635 \left(\frac{b}{1.3 \text{ km s}^{-1}} \right) \left[1 + 0.194 \ln \left(\frac{b}{1.3 \text{ km s}^{-1}} \right) \right] \\ &= 931 \left(\frac{b}{10 \text{ km s}^{-1}} \right) \left[1 + 0.139 \ln \left(\frac{b}{10 \text{ km s}^{-1}} \right) \right] \end{aligned}$$

$$[N_{\ell}]_{\text{damp}} \approx \frac{4m_e c}{e^2} \frac{b^2}{f_{\ell u} \gamma_{\ell u} \lambda_{\ell u}^2} \ln \left[\frac{4\sqrt{\pi}}{\ln 2} \frac{b}{\gamma_{\ell u} \lambda_{\ell u}} \right]$$

$$[N_{\ell}]_{\text{damp}} = 1.23 \times 10^{16} [\text{cm}^{-2}] \left(\frac{0.4164}{f_{\ell u}} \right) \left(\frac{1215.67 \text{ \AA}}{\lambda_{\ell u}} \right) \left(\frac{b}{10 \text{ km s}^{-1}} \right) \left(\frac{\tau_{\text{damp}}}{931} \right)$$

Approximate Formulae for W

- Rodgers & Williams (1974, JQSRT, 14, 319) give a simple approximation.

$$W \approx [W_L^2 + W_D^2 - (W_L W_D / W_W)^2]^{1/2}$$

W_L = EW of the Lorentz-broadened line (damped portion)

W_D = EW of the Doppler-broadened line (flat portion)

$W_W = \tau_0$ is the weak limit for a line of any shape

- B. T. Draine (2011) provides a simple approximation that is continuous and accurate to a few percent for all τ_0 when applied to H I Ly α with $b = 10$ km/s.

$$W \approx \begin{cases} \sqrt{\pi} \frac{b}{c} \frac{\tau_0}{1+\tau_0/(2\sqrt{2})} & \text{for } \tau_0 < 1.25393 \\ \left[\left(\frac{2b}{c} \right)^2 \ln \left(\frac{\tau_0}{\ln 2} \right) + \frac{b}{c} \frac{\gamma_{\ell u} \lambda_{\ell u}}{c} \frac{(\tau_0 - 1.25393)}{\sqrt{\pi}} \right]^{1/2} & \text{for } \tau_0 > 1.25393 \end{cases}$$

Note that

$$W_D \approx \frac{2b}{c} \sqrt{\ln (\tau_0 / \ln 2)}$$

$$W_L \approx \sqrt{\frac{b}{c} \frac{\tau_0}{\sqrt{\pi}} \frac{\gamma_{\ell u} \lambda_{\ell u}}{c}}$$

Observations: H and D Ly α

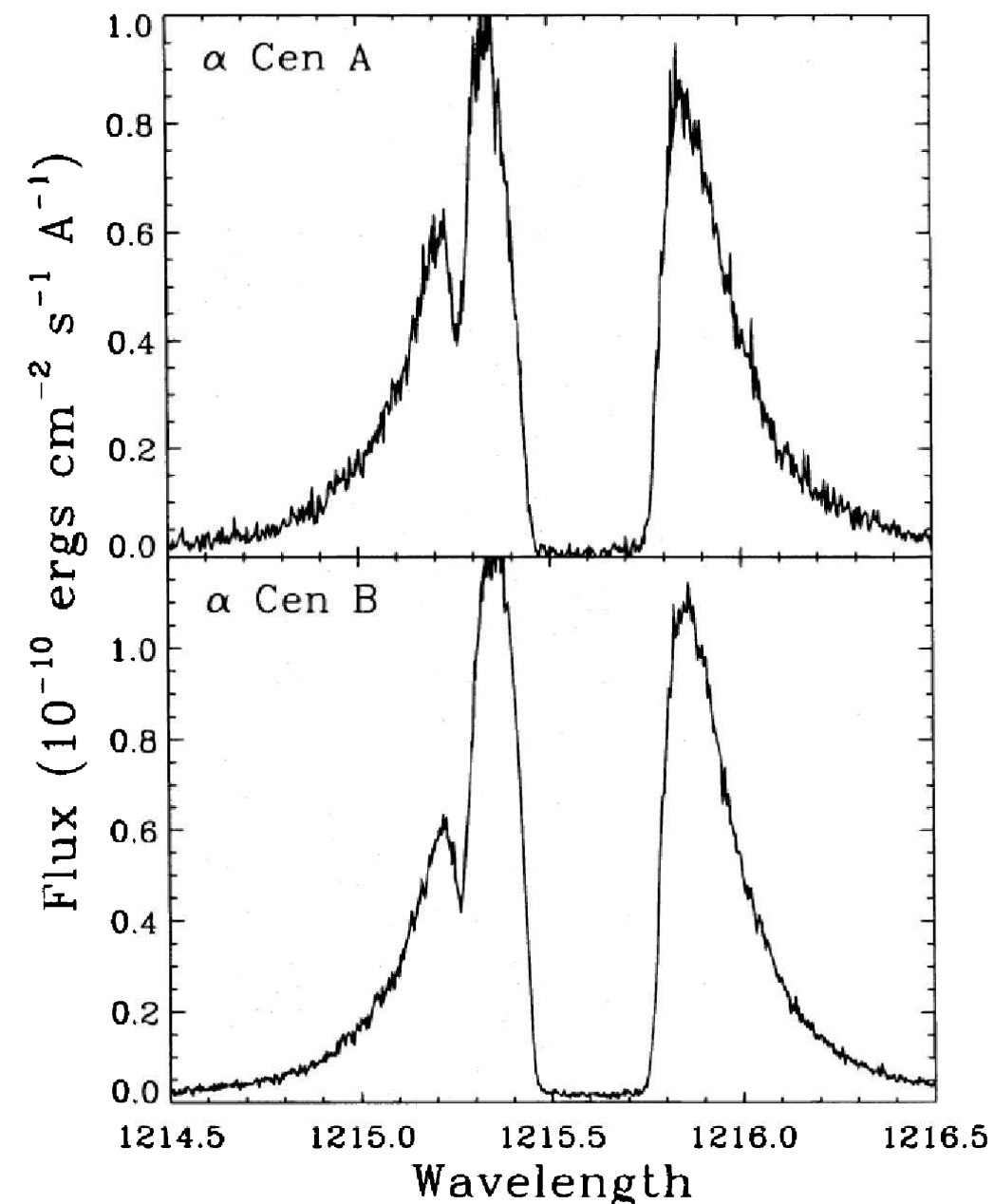
- The study of Ly α absorption line is useful to studying the cold clouds in our galaxy. However, Ly α tends to be optically thick.
- α Cen A and B ($d = 1.34$ pc) have broad Ly α “emission” lines from their hot chromospheres.
 - Superposed on the emission lines are optically thick absorption lines by the ISM.
 - For both α Cen A and B, $W_\lambda = 0.3 \text{ \AA}$.

$$\tau_0 = 68,000, b = 11.8 \text{ km s}^{-1} (T = 8300 \text{ K})$$

$$N_\ell = 1.1 \times 10^{18} \text{ cm}^{-2}$$

- This represents the regime where the flat part of the curve of growth gives way to the square-root part. Hence, the column density is independent of the thermal broadening.
- The stars are within our Local “Hot” Bubble so that the temperature is high. The column density imply that a density of 0.27 cm^{-3} .

$$n_{\text{H}} = N_{\text{H}}/d = 1.1 \times 10^{18} \text{ cm}^{-2}/1.34 \text{ pc} \quad (1 \text{ pc} = 3.1 \times 10^{18} \text{ cm})$$



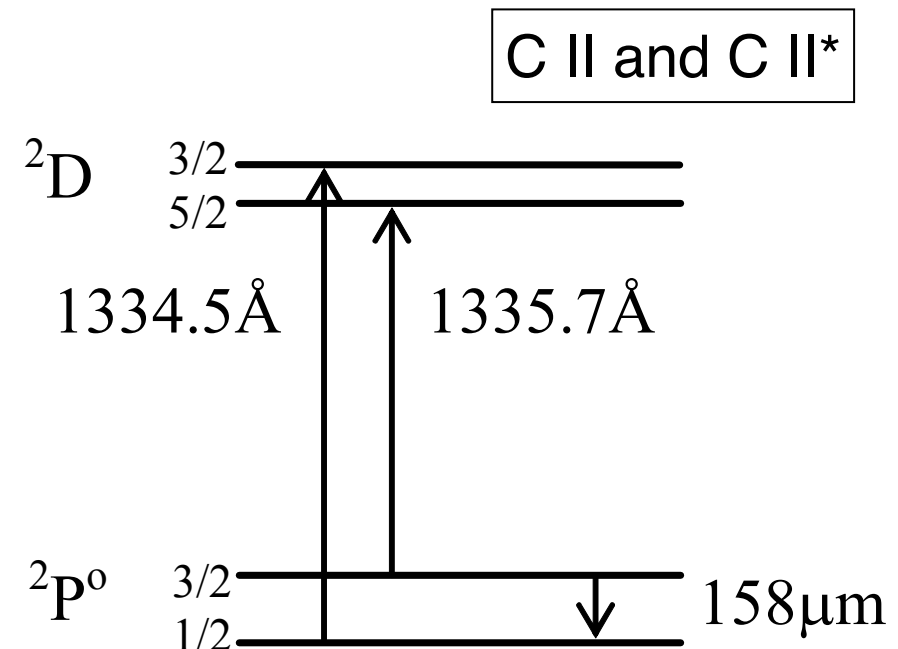
Ly α lines toward α Cen A (above) and α Cen B (below).

Figure 2.8 in [Ryden], (Linsky & Wood 1996)

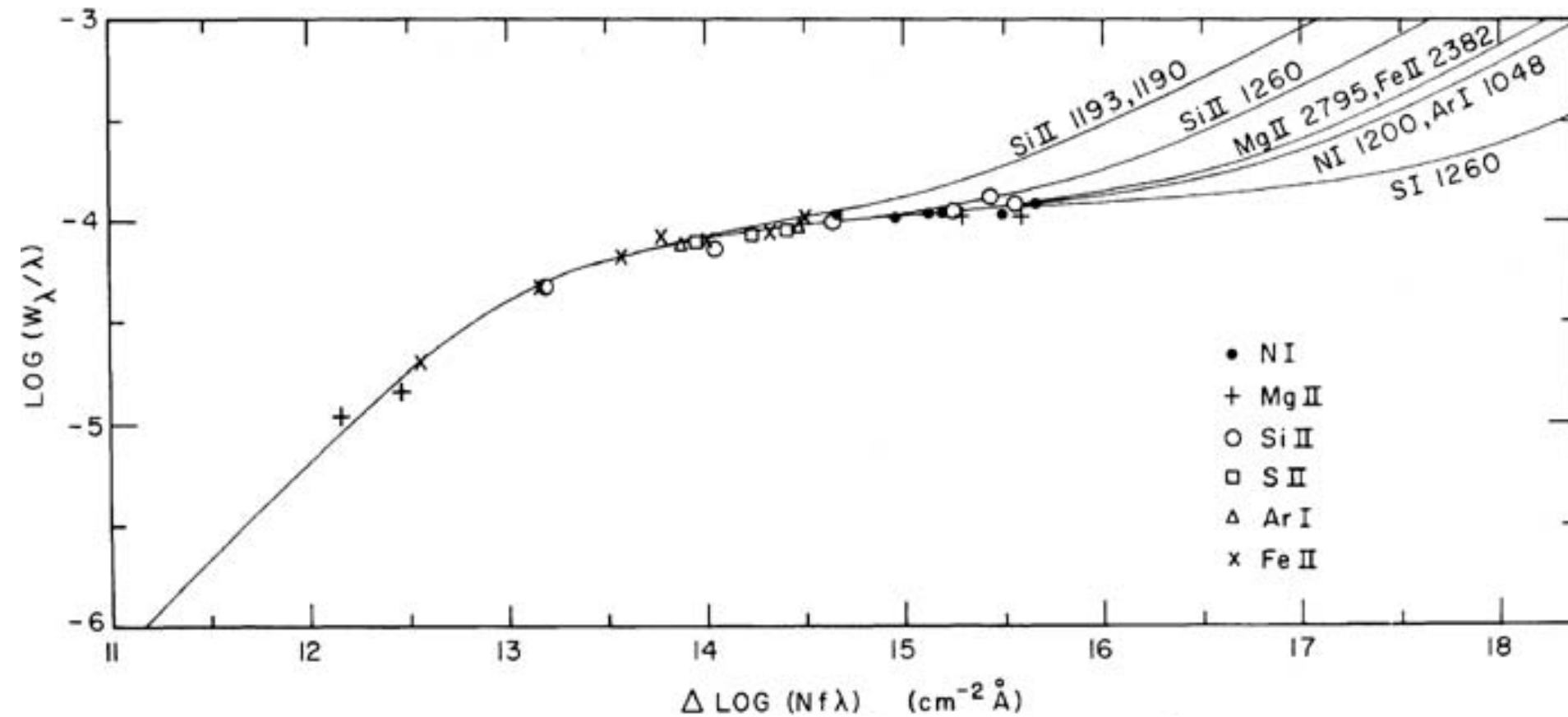
-
- On the left-hand slope of the Ly α emission lines, there is an optically thin absorption line. This is the absorption line of **deuterium** Ly α .
 - ▶ The deuterium Ly α lines are slightly blueshifted. wavelength for H Ly α = 1215.67Å, wavelength for deuterium Ly α is 1215.24Å.
 - ▶ The deuterium Ly α lines are optical thin, with $\tau_0 = 0.68$, and thus easier to interpret than the H Ly α from ordinary hydrogen. The column density of deuterium toward α Cen A and B, is $N_\ell = 6.1 \times 10^{12} \text{ cm}^{-2}$, giving a deuterium to hydrogen ratio $D/H \approx 6 \times 10^{-6}$. This is lower than the usual $D/H \approx 1.6 \times 10^{-5}$ in the Local Bubble, and is much less than the primordial value of $D/H \approx 2.5 \times 10^{-5}$.
 - For stars outside the Local Bubble, at $d \sim 100 \text{ pc}$, Ly α lines are in the square-root part of the curve of growth, with $W_\lambda \sim 10 \text{ \AA}$, $N_\ell \sim 2 \times 10^{20} \text{ cm}^{-2}$, $n_\ell \sim 0.6 \text{ cm}^{-3}$.
 - We observe in the visible and UV spectrum of many stars a substantial number of atomic interstellar absorption lines.
 - The coexistence of Ca⁰ and Ca⁺ lines also allows us to obtain the degree of ionization of the corresponding cloud. We observe that Ca⁺ is much more abundant than Ca⁰ (ionization potential of Ca is 6.11 eV).

Observations: Absorption lines from fine-structure levels

- We also observe several absorption lines with wavelength close to each other, which comes from fine-structure levels of the fundamental ground state of the same atom or ion.
 - We can then directly obtain the relative populations of these levels. This gives valuable information on those physical parameters that determine their excitation, essentially the electron density.
 - For example, C II 1334.57Å and C II* 1335.70Å lines, which unfortunately are often saturated.
 - Morton (1975)'s observations of the C II and C II* ratio showed a significant population of atoms in $^2P_{3/2}^o$. This suggested that [C II] 157.7 μm line could be a strong cooling line in H I regions. It was not until the 1980s that the Kuiper Airborne Observatory detected Far-IR [C II] emission from the ISM, as predicted by Morton.
 - We may determine the cooling rate of the diffuse CNM due to [C II] 157.7 μm by observing the C II* 1335.70Å absorption line.
 - This observation gave a cooling rate of $\sim 3.5 \times 10^{-26}$ erg s⁻¹ per hydrogen nucleus (Pottasch et al. 1979; Gry et al. 1992), which is in agreement with the more direct determination of Bennett et al. (1994) using [C II] 157.7 μm.



- Observed curve of growth for the ISM in front of the star ζ Oph (Morton 1975, ApJ)



- As can be seen in the above figure, most observed absorption lines lie on the Doppler plateau.
- Therefore, a better reduction technique than the use of curves of growth would be to adopt a fitting technique for the line profiles. This technique is the only one that can be used for complex line profiles.
- So, optical and UV absorption lines provide us useful information about the cold regions in the ISM. How much of each element and isotope is present? How hot is the gas? What are the integrated densities along the line of sight?

Observations: The Gas Phase Abundances

- The gas phase abundances of many elements relative to hydrogen have been determined on many different sightlines using interstellar absorption lines.
 - The observed gas-phase abundances vary from one sightline to another, which is presumed to reflect primarily variations in the amounts of various elements trapped in dust grains. Such removal of elements from the gas is known as ***interstellar depletion***.
 - Some elements, like Fe, are extremely under abundant in the gas phase, with gas-phase abundances that are typically only a few percent of the solar abundance.

Element	Solar system 12 + log(X/H)	Stars	H II	T_c^1 K	ζ Oph cold [X/H]	ζ Oph warm [X/H]
H	12.00	12.00	12.00	–	–	–
D	7.53	–	–	–	-0.33: ²	
He	10.99	–	10.95	–	–	–
Li	3.31	–	–	1 225	-1.58	–
B	2.88	–	–	650	-0.93	–
C	8.55	8.33	8.60	75	-0.41	–
N	7.97	7.82	7.89	120	-0.07	–
O	8.87	8.66	8.77	180	-0.39	0.00
Ne	–	–	8.03	–	–	–
Na	6.31	–	–	970	-0.95	–
Mg	7.58	7.40	–	1 340	-1.55	-0.89
Si	7.55	7.27	–	1 311	-1.31	-0.53
P	5.57	–	–	1 151	-0.50	-0.23
S	7.27	7.09	7.31	648	+0.18	–
Ar	6.56	–	–	25	-0.48	–
K	5.13	–	–	1 000	-1.09	–
Ca	6.34	6.20	–	1 518	-3.73	–
Ti	4.93	4.81	–	1 549	-3.02	-1.31
Fe	7.50	7.43	6.59	1 336	-2.27	-1.25

¹ Condensation temperature at thermal and chemical equilibrium, appropriate for the Solar nebula with an initial gas pressure of 10^{-4} bar. ($1 \text{ bar} = 10^6 \text{ dyn cm}^{-2}$)

² For lines of sight other than that of ζ Oph: Linsky et al. (1995).

The gas phase abundances along two lines of sight, compared to abundances in the Solar system.

Abundances are given as $12 + \log(X/H)$, X being the chemical symbol for the element and H that of hydrogen.

The deficiencies in columns 6 and 7 are expressed as:

$$[X/H] = \log(X/H) - \log(X/H)_\odot$$

The data come mainly from Savage & Sembach (1996) and from Snow & Witt (1996).

Gas-phase abundance vs. Condensation Temperature

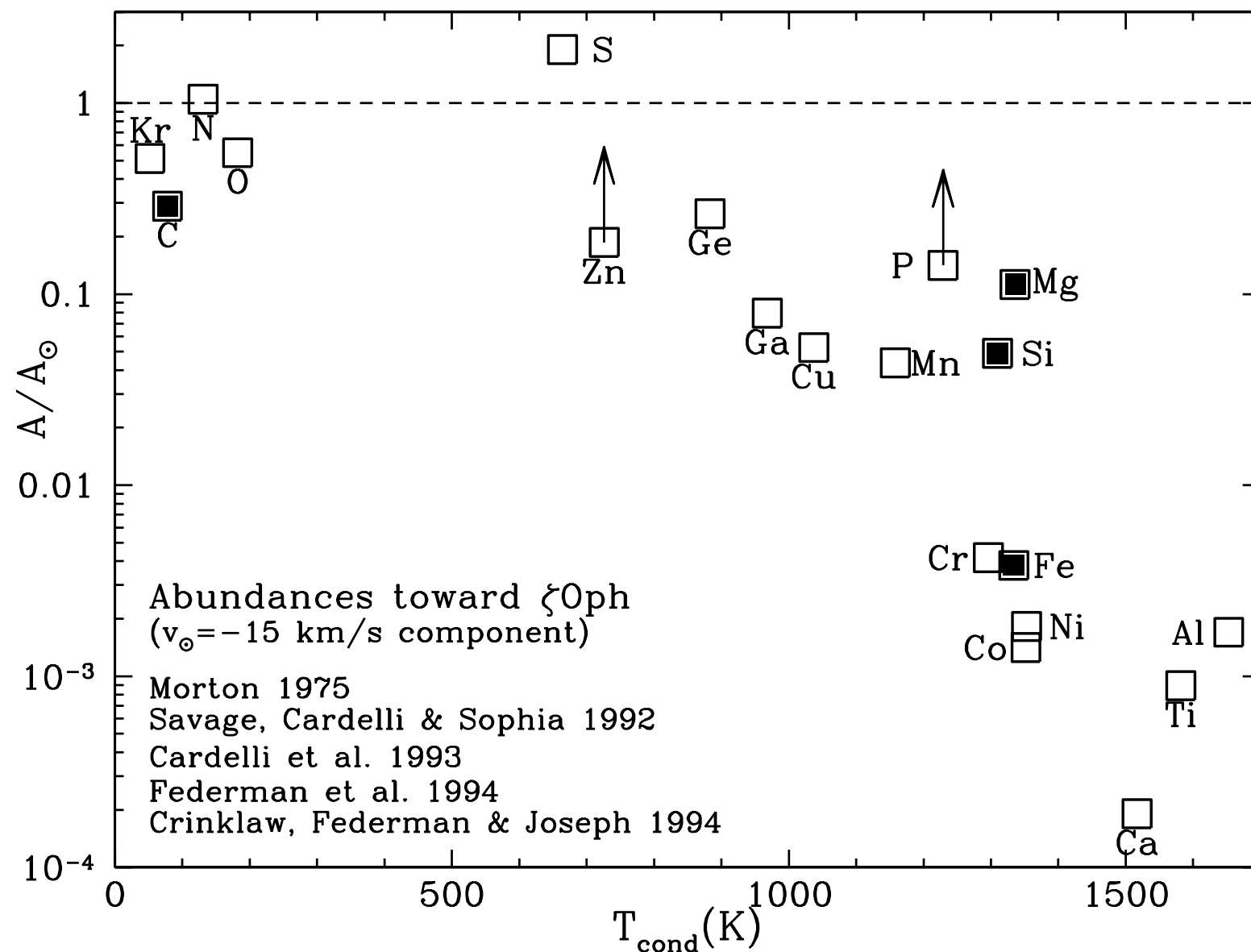


Figure 23.1 in [Draine]

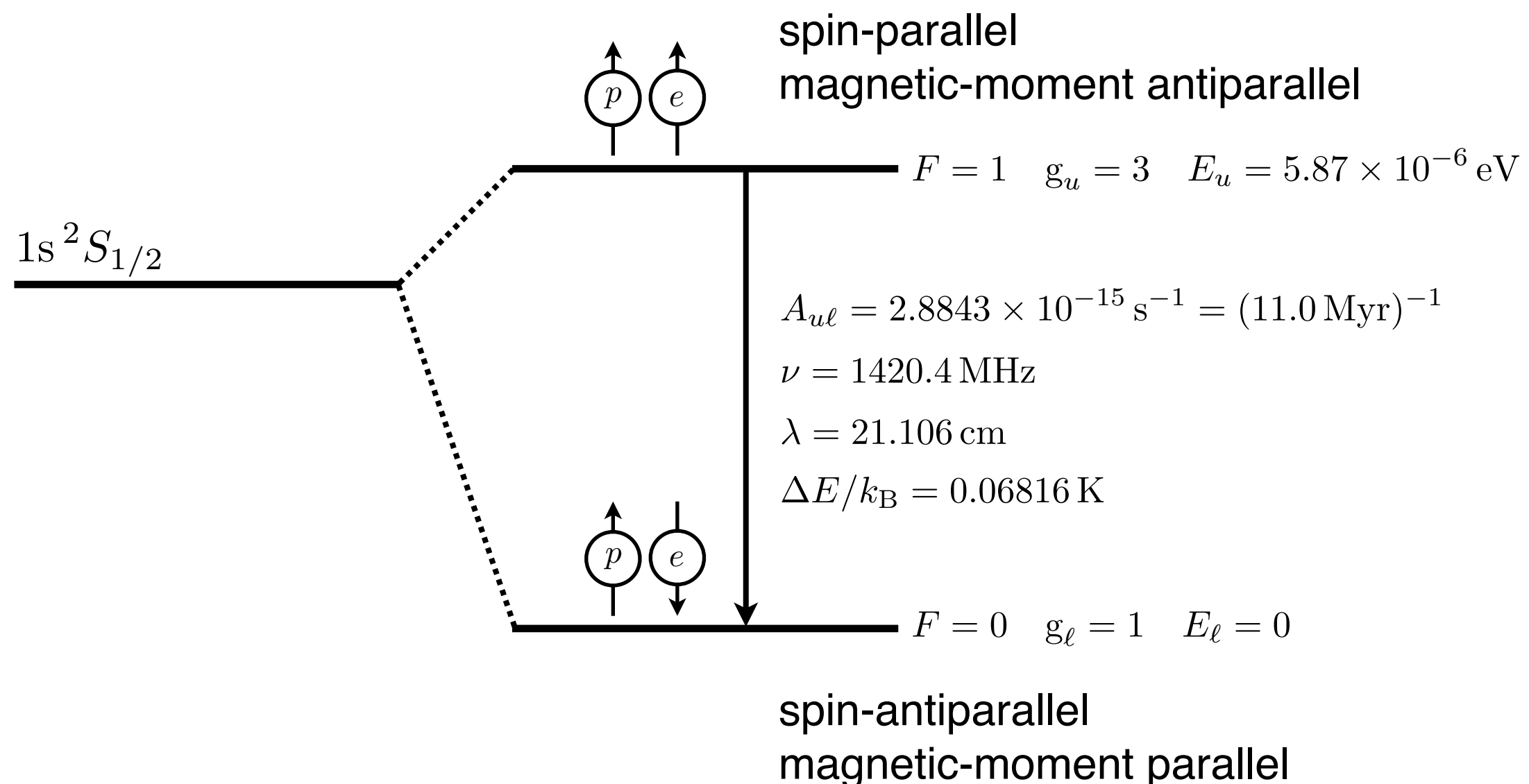
Gas-phase abundances (relative to solar) in the diffuse cloud toward ζ Ophiuchi (O9.5V star, 138 pc), plotted versus “condensation temperature”. Solid symbols: major grain constituents C, Mg, Si, Fe. The apparent overabundance of S may be due to observational error, but may arise because of S II absorption in the H II region around ζ Oph. There’s a strong tendency for elements with high condensation temperature (T_{cond}) to be under abundant in the gas phase, presumably because most of the atoms are in solid grains.

Condensation temperature : temperature at which 50% of the element in question would be incorporated into solid material in a gas of solar abundances, at LTE at a pressure $p = 10^2 \text{ dyn cm}^{-2}$ (Lodders 2003).

21 cm hyperfine line

- **The CNM and WNM, taken together, provide over half the mass of the ISM.**
 - H is the most abundant element in the universe. In the CNM and WNM, most of the hydrogen is in the form of neutral atoms.
 - The Ly α line of H provides a useful probe of the properties of the CNM and WNM. However, at its wavelength the Earth's atmosphere is highly opaque, and thus observing Ly α absorption requires orbiting UV satellites. In addition, Ly α can be seen in absorption only along those lines of sight toward sources with a high UV flux.
- *To do a global survey of atomic hydrogen in the galaxy, we need some way of easily detecting radiation from hydrogen, regardless of its kinetic temperature or number density.*
- Such a way was first found in 1944, by Henk van de Hulst.
 - ▶ He attempted to find emission lines at the wavelengths ~ 1 cm to 20 m, at which the Earth's atmosphere is transparent. He then realized that the hyperfine structure line resulting from a flip of the electron spin within a hydrogen atom should have a wavelength of 21 cm.
 - ▶ This was confirmed by Harold Ewen and Edward Purcell in 1951, when they first detected 21 cm emission from the Milky Way.

Hyperfine splitting of the 1s ground state of atomic H



Note that the magnetic moment is proportional to the charge, so the electron and proton have opposite directions of the magnetic moments.

Difference between Ly α and 21 cm transitions

- The excitation energy for Ly α ($E = 10.2 \text{ eV}$, $E/k_B = 118,000 \text{ K}$) is much higher than the kinetic temperature of the neutral ISM.

$$\frac{n_u}{n_\ell} = \frac{g_u}{g_\ell} \exp\left(-\frac{118,000 \text{ K}}{T}\right) = 1.7 \times 10^{-51} \text{ at } T = 1000 \text{ K}$$

- Collisional excitation is unimportant, and most hydrogen atoms are in the lower level of the Ly α transition.
- The Ly α has a higher energy by a factor of 1.7×10^6 than the 21 cm.
- The excitation energy for 21 cm is $\sim 5.9 \mu\text{eV}$, and its equivalent temperature $E/k_B = 0.068 \text{ K}$ is much lower than the temperature of the cosmic microwave background.
 - ***Even the CMB is able to populate the upper level.***
 - ***If collisions are frequent, then the spin temperature will be solely determined by collisions, and thus will be a good tracer of the gas kinetic temperature.***
 - Thus, there is ample opportunity to populate the upper energy level of the 21 cm hyperfine transition. The level populations for the 21 cm levels, since $T_{\text{exc}} \gg 0.068 \text{ K}$ in all circumstances of the ISM will be:

$$\frac{n_u}{n_\ell} = \frac{g_u}{g_\ell} e^{-h\nu/kT_{\text{exc}}} = 3 e^{-0.068 \text{ K}/T_{\text{exc}}} \simeq 3 \longrightarrow n_u \simeq \frac{3}{4} n_H, \quad n_\ell \simeq \frac{1}{4} n_H$$

- However, in many cases (in particular in WNM), the hyperfine levels may not be in excitation equilibrium. Radio astronomers use the term ***spin temperature*** for 21 cm rather than the “excitation temperature.”

Emissivity and Optical Depth of H I 21 cm

- **Emissivity:**

- The upper level contains $\sim 75\%$ of the H I under all conditions of interest, and thus *the 21-cm emissivity is effectively independent of the spin temperature.*

$$j_\nu = n_u \frac{A_{ul}}{4\pi} h\nu_{ul} \phi_\nu \simeq \frac{3}{16\pi} A_{ul} h\nu_{ul} n_H \phi_\nu \quad \left(n_u \simeq \frac{3}{4} n_H \right)$$

- **Optical depth**

$$\kappa_\nu = n_\ell \sigma_{\ell u} - n_u \sigma_{ul} = n_\ell \sigma_{\ell u} \left(1 - e^{-h\nu_{ul}/kT_{\text{spin}}} \right)$$

Because $h\nu_{ul}/kT_{\text{spin}} \ll 1$ for all conditions of interest, the correction for stimulated emission is very important!

$$\kappa_\nu \simeq n_\ell \sigma_{\ell u} \frac{h\nu_{ul}}{kT_{\text{spin}}} \ll n_\ell \sigma_{\ell u} \quad \longleftarrow \quad e^{-h\nu_{ul}/kT_{\text{spin}}} \simeq 1 - k\nu_{ul}/kT_{\text{spin}}$$

$$\kappa_\nu \simeq \left(\frac{1}{4} n_H \right) \left(\frac{g_u}{g_\ell} \frac{c^2}{8\pi\nu_{ul}^2} A_{ul} \phi_\nu \right) \frac{h\nu_{ul}}{kT_{\text{spin}}} \quad \longleftarrow \quad \left(n_\ell \simeq \frac{1}{4} n_H \right)$$

$$\kappa_\nu \simeq \frac{3}{32\pi} A_{ul} \frac{hc \lambda_{ul}}{kT_{\text{spin}}} n_H \phi_\nu \quad \longleftarrow \quad \frac{g_u}{g_\ell} = 3$$

The absorption coefficient is inversely proportional to the spin temperature.

- The damping constant of the 21 cm line profile is extremely small, and thus we can assume that the line profile is a Gaussian.

$$a = \frac{\gamma_{u\ell}}{4\pi} \frac{\lambda_{u\ell}}{b} = 4.844 \times 10^{-20} \left(\frac{\gamma_{u\ell}}{2.8843 \times 10^{-15} \text{ s}^{-1}} \right) \left(\frac{\lambda_{u\ell}}{21.106 \text{ cm}} \right) \left(\frac{1 \text{ km s}^{-1}}{b} \right)$$

- Hence,

$$\phi_\nu = \frac{1}{\sqrt{\pi} \Delta \nu_D} H(u, a) \simeq \frac{c}{\sqrt{\pi} \nu_{\ell u} b} e^{-u^2} \quad \left(u = v/b, \ b = \sqrt{2} v_{\text{rms}} = \sqrt{2 k T_{\text{gas}} / m_{\text{H}}} \right)$$

$$\tau_\nu = \kappa_\nu s = \frac{3}{32\pi} A_{u\ell} \frac{hc \lambda_{u\ell}}{kT_{\text{spin}}} N_{\text{HI}} \phi_\nu \quad N_{\text{HI}} \equiv \int n_{\text{H}} ds \text{ is the column density of HI.}$$

$$= \frac{3}{32\pi} \frac{1}{\sqrt{\pi}} \frac{A_{u\ell} \lambda_{u\ell}^2}{b} \frac{hc}{kT_{\text{spin}}} N_{\text{HI}} e^{-u^2} \quad \sim 10^{21} \text{ cm}^{-21} \text{ toward the Galactic disk.}$$

$$\tau_\nu = 3.111 \left(\frac{N_{\text{HI}}}{10^{21} \text{ cm}^{-2}} \right) \left(\frac{100 \text{ K}}{T_{\text{spin}}} \right) \left(\frac{1 \text{ km s}^{-1}}{b} \right) e^{-u^2}$$

$$\text{or } \tau_\nu = 2.201 \left(\frac{N_{\text{HI}}}{10^{21} \text{ cm}^{-2}} \right) \left(\frac{100 \text{ K}}{T_{\text{spin}}} \right) \left(\frac{1 \text{ km s}^{-1}}{b/\sqrt{2}} \right) e^{-u^2}$$

Some lines of sight through our galaxy (at high galactic latitude) are optically thin and other lines of sight (at low galactic latitude) are optically thick at 21 cm.

- Self-absorption in the 21-cm line can be important** in many sightlines in the ISM.
- The optical depth is inversely proportional to the spin temperature.**

- Typical optical depths of the 21-cm line:

$$\tau_0 = 0.311 \left(\frac{N_{\text{HI}}}{10^{21} \text{ cm}^{-2}} \right) \left(\frac{100 \text{ K}}{T_{\text{spin}}} \right) \left(\frac{10 \text{ km s}^{-1}}{b} \right)$$

- In the CNM, a typical spin temperature is $T_{\text{spin}} \approx 50 - 100 \text{ K}$:

$$\tau_0^{\text{CNM}} \approx 0.3 - 0.6$$

$$e^{-\tau_0} \approx 0.55 - 0.74$$

The CNM is in general optically thin, but show significant absorption.

- In the WNM, a typical spin temperature is $T_{\text{spin}} \approx 5000 - 8000 \text{ K}$:

$$\tau_0^{\text{WNM}} \approx 0.004 - 0.006$$

$$e^{-\tau_0} \approx 0.995$$

The 21-cm absorption is negligible in the WNM.

A typo in page 59 of Ryden's book: For thermal broadening b values typical of the ~~warm~~^{cold} neutral medium and excitation temperatures $T_{\text{exc}} \sim 100 \text{ K}$, lines of sight with $N_{\text{HI}} > 10^{21} \text{ cm}^{-2}$ show significant absorption. (Remember from Section 2.3 that Lyman α becomes

[1] Column Density Determination - Emission

- Radio astronomers express the line profile as a function of radial velocity rather than of frequency.** This is logical because line broadening is only caused by the Doppler effect, and its natural width being extremely narrow since the lifetime of the upper level is only limited by collisions which are rare in the diffuse medium.
- We first define the column density per velocity interval.

$$\frac{dN_{\text{HI}}}{dv} = N_{\text{HI}}\phi_v = N_{\text{HI}} \frac{1}{\lambda_{u\ell}} \phi_\nu \quad \phi_\nu = \phi_v \left| \frac{dv}{d\nu} \right| = \phi_v \frac{c}{\nu_{u\ell}} = \lambda_{u\ell} \phi_v$$

- The column density can be written:

$$\tau_\nu = \frac{3}{32\pi} A_{u\ell} \frac{hc \lambda_{u\ell}}{kT_{\text{spin}}} N_{\text{HI}} \phi_\nu \rightarrow \tau(v) = \frac{3}{32\pi} A_{u\ell} \frac{hc \lambda_{u\ell}^2}{kT_{\text{spin}}(v)} \frac{dN_{\text{HI}}}{dv}$$

$$\begin{aligned} \frac{dN_{\text{HI}}}{dv} &= \frac{32\pi}{3} \frac{k}{A_{u\ell} hc \lambda_{u\ell}^2} T_{\text{spin}}(v) \tau(v) \\ &= 1.813 \times 10^{18} \frac{T_{\text{spin}}(v) \tau(v)}{\text{K}} \left[\frac{\text{cm}^{-2}}{\text{km s}^{-1}} \right] \end{aligned} \quad N_{\text{HI}} = \int dv \frac{dN_{\text{HI}}}{dv}$$

- This indicates that **we need to know not only the optical depth but also the spin temperature to evaluate the column density**. However, **in an optically thin limit, we will show that the dependency on the spin temperature is removed**.

- **Optically thin case:** Suppose we are looking through an optically thin layer of neutral hydrogen toward a “**dark sky**”, which is fainter than the hydrogen cloud, with an antenna temperature T_{sky} .
 - In the optically thin limit, the RT equation becomes

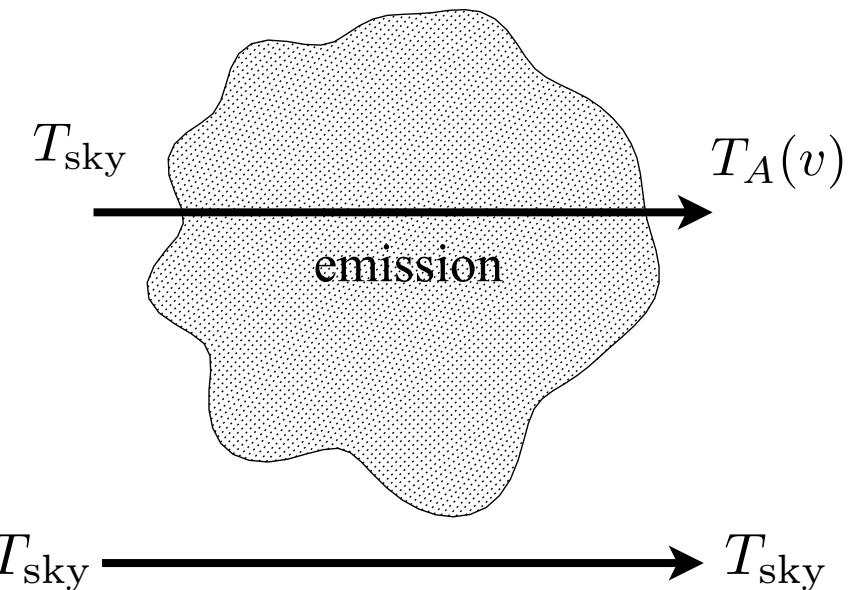
$$\begin{aligned} T_A(v) &= T_{\text{sky}} e^{-\tau_v} + T_{\text{spin}}(v) (1 - e^{-\tau_v}) \\ &= T_{\text{sky}} + (T_{\text{spin}}(v) - T_{\text{sky}}) (1 - e^{-\tau_v}) \\ &\approx T_{\text{sky}} + T_{\text{spin}}(v) \tau_v \quad \leftarrow \tau_v \ll 1, \quad T_{\text{sky}} \ll T_{\text{spin}}(v) \end{aligned}$$

$$\tau(v) \approx \frac{T_A(v) - T_{\text{sky}}}{T_{\text{spin}}(v)} \approx \frac{T_A(v)}{T_{\text{spin}}(v)}$$

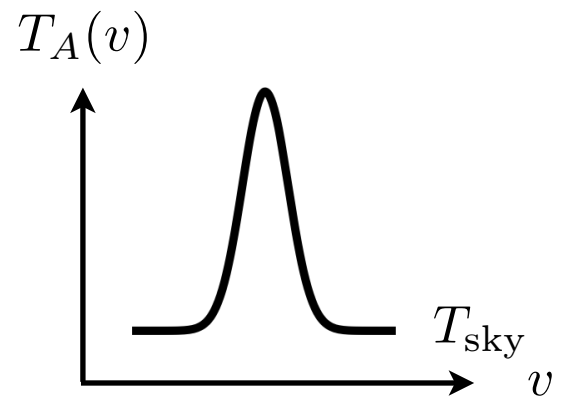
- The column density per unit velocity interval is

$$\begin{aligned} \frac{dN_{\text{HI}}}{dv} &\approx \frac{32\pi}{3} \frac{k}{A_{u\ell} h c \lambda_{u\ell}^2} [T_A(v) - T_{\text{sky}}] \\ &= 1.813 \times 10^{18} \frac{T_A(v) - T_{\text{sky}}}{\text{K}} \left[\frac{\text{cm}^{-2}}{\text{km s}^{-1}} \right] \end{aligned}$$

$$N_{\text{HI}} = \int dv \frac{dN_{\text{HI}}}{dv}$$



We measure the antenna temperature of the dark sky (T_{sky}) from the continuum at frequencies well above and below the 21-cm emission feature.



- Therefore, *the intensity integrated over the line profile gives us the total H I column density without need to know T_{spin} , provided that self-absorption is not important.*

- **Alternative approach:**

- If we now neglect absorption, then

$$\frac{dI_\nu}{ds} = -\kappa_\nu I_\nu + j_\nu \approx j_\nu$$



$$\begin{aligned} I_\nu &= I_\nu(0) + \int j_\nu ds \\ &= I_\nu(0) + \frac{3}{16\pi} A_{u\ell} h \nu_{u\ell} \phi_\nu N_{\text{HI}} \end{aligned}$$

- Now suppose that $I_\nu(0)$ is known independently. We can then integrate the intensity over the line

$$\int [I_\nu - I_\nu(0)] d\nu = \frac{3}{16\pi} A_{u\ell} h \nu_{u\ell} N_{\text{HI}}$$

- This can be expressed in terms of antenna temperature T_A and relative velocity $v = [(\nu - \nu_{u\ell})/\nu_{u\ell}] c$

$$\begin{aligned} \int [T_A - T_A(0)] dv &= \int \frac{c^2}{2k\nu^2} [I_\nu - I_\nu(0)] \frac{c}{\nu_{u\ell}} d\nu \\ &\approx \frac{c^3}{2k\nu_{u\ell}^3} \frac{3}{16\pi} A_{u\ell} h \nu_{u\ell} N_{\text{HI}} \\ &= C_0^{-1} N_{\text{HI}} \end{aligned}$$

$$\begin{aligned} C_0 &\equiv \frac{32\pi}{3} \frac{k}{hc\lambda_{u\ell}^2 A_{u\ell}} \\ &= 1.813 \times 10^{18} \left[\frac{\text{cm}^{-2}}{\text{K km s}^{-1}} \right] \\ C_0^{-1} &= 5.516 \times 10^{-19} \left[\frac{\text{K km s}^{-1}}{\text{cm}^{-2}} \right] \end{aligned}$$

-
- We, then, obtain the same equation as before:

$$\begin{aligned} N_{\text{HI}} &\approx C_0 \int [T_A - T_A(0)] dv \\ &= 1.813 \times 10^{18} \int \frac{T_A - T_A(0)}{\text{K km s}^{-1}} dv \quad [\text{cm}^{-2}] \end{aligned}$$

- Here, we did not use the relation between the optical depth and column density.
 - In the first method, we assumed that $\tau_\nu \ll 1$ and $I_\nu(0) \ll S_\nu$:

$$\begin{aligned} I_\nu &= I_\nu(0)e^{-\tau_\nu} + S_\nu (1 - e^{-\tau_\nu}) \\ &= I_\nu(0) + [S_\nu - I_\nu(0)] (1 - e^{-\tau_\nu}) \\ &\approx I_\nu(0) + S_\nu \tau_\nu \end{aligned}$$

- In the second method, we completely ignored the absorption.

$$\frac{dI_\nu}{ds} = -\kappa_\nu I_\nu + j_\nu \approx j_\nu$$

Integrating the above equation, we obtain the same result as in the first method.

$$I_\nu \approx I_\nu(0) + j_\nu \int ds = I_\nu(0) + S_\nu \tau_\nu$$

[2] Spin Temperature Determination - Emission & Absorption

- To derive the spin temperature, **we need to combine the emission observation with an absorption observation**, which is so called **“emission-absorption” method**.

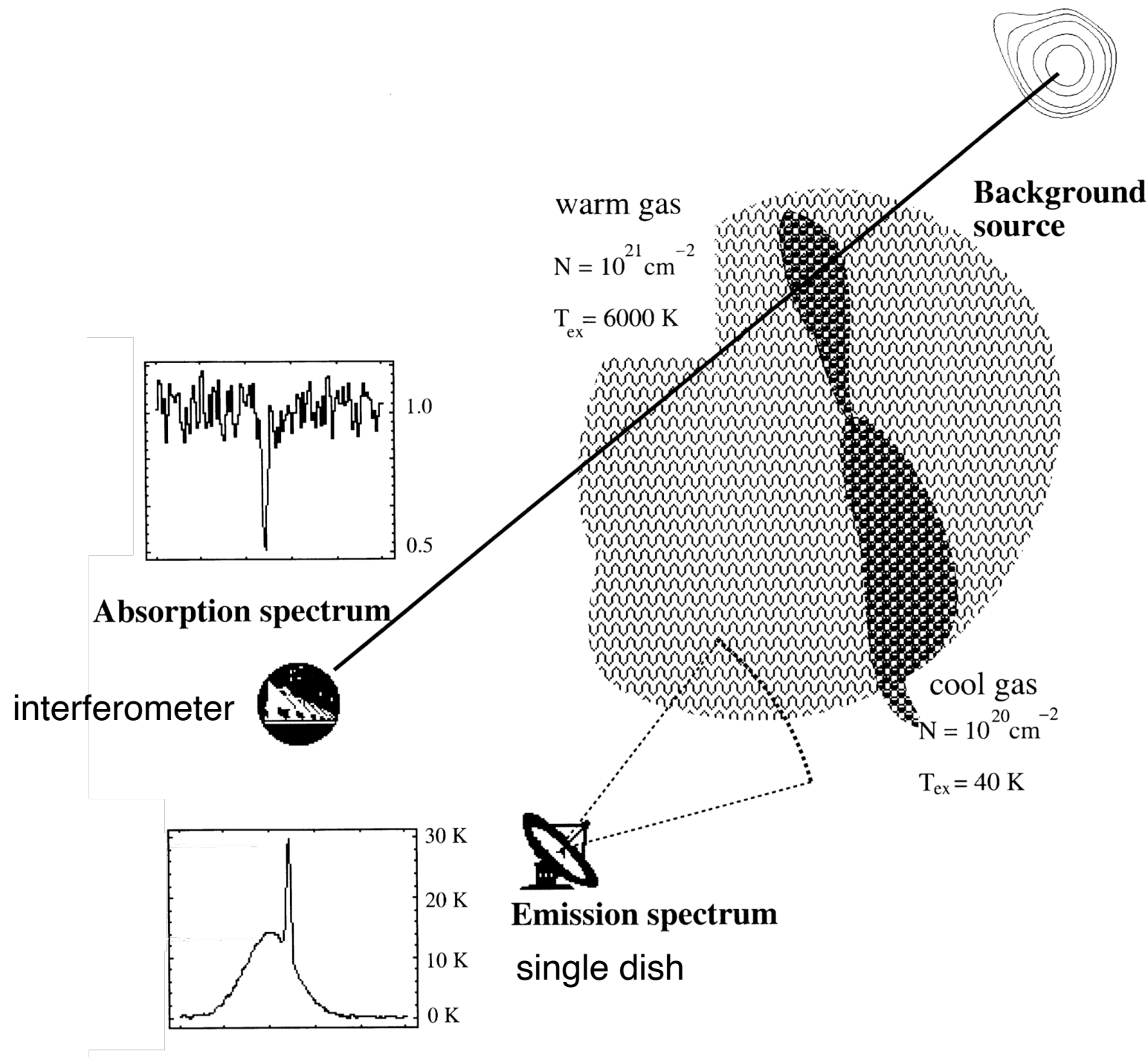


Figure 15 in Dickey et al. (2000, ApJ)

- In cases where we have a “**bright background radio source**” with a continuum spectrum (a typical radio-loud quasar or an active galactic nucleus, or a radio galaxy), we can study both emission and absorption by the foreground ISM in our galaxy by comparing “**on-source**” and “**off-source**” observations.
- The spectra measured on the blank sky and on the radio source are, respectively,

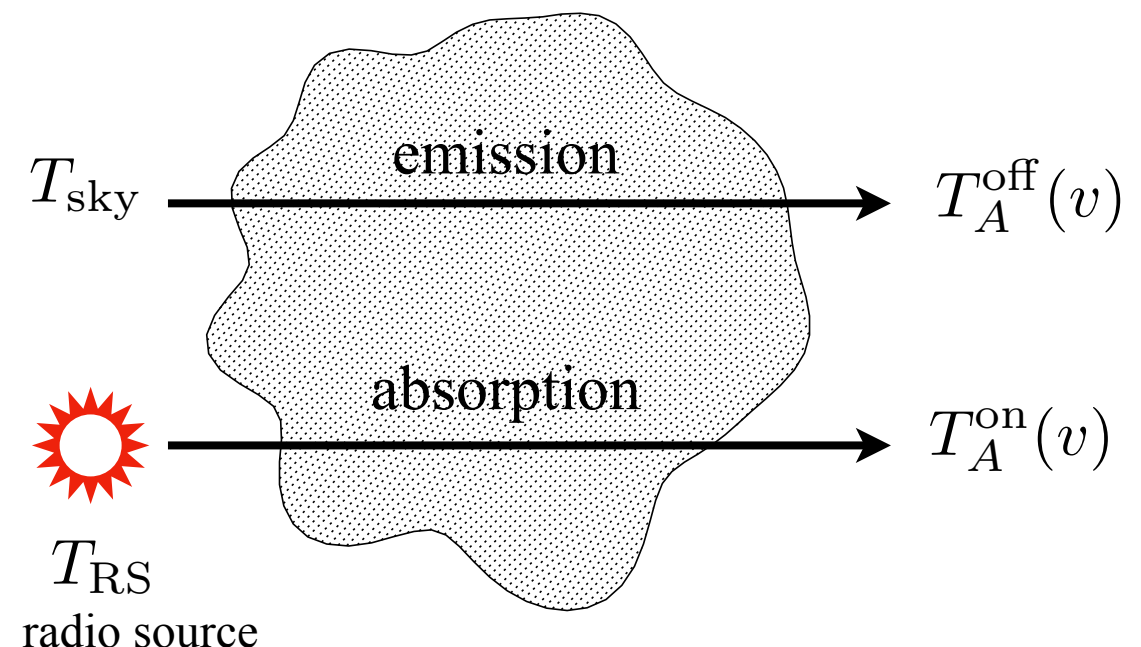
$$T_A^{\text{on}}(v) = T_{\text{RS}} e^{-\tau_v} + T_{\text{spin}}(v) (1 - e^{-\tau_v})$$

$$T_A^{\text{off}}(v) = T_{\text{sky}} e^{-\tau_v} + T_{\text{spin}}(v) (1 - e^{-\tau_v})$$

- These two equations can be solved for the two unknowns, $\tau(v)$ and $T_{\text{spin}}(v)$.

$$\tau(v) = \ln \left[\frac{T_{\text{RS}} - T_{\text{sky}}}{T_A^{\text{on}}(v) - T_A^{\text{off}}(v)} \right]$$

$$T_{\text{spin}}(v) = \frac{T_A^{\text{off}}(v)T_{\text{RS}} - T_A^{\text{on}}(v)T_{\text{sky}}}{(T_{\text{RS}} - T_{\text{sky}}) - [T_A^{\text{on}}(v) - T_A^{\text{off}}(v)]}$$



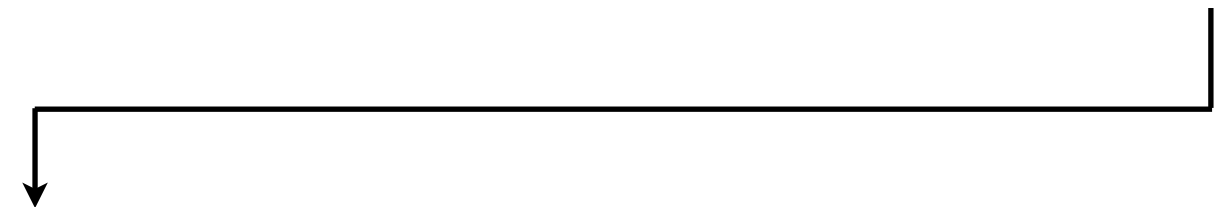
The solutions give, in general, the spin temperature and the column density as functions of velocity.

We can derive the column density from these two quantities for an optically thick cloud.

- We usually consider a case where ***the radio source is “much” brighter than the spin temperature of the intervening hydrogen cloud.***
 - The RT equations for the “on-source” and “off-source” measurements can be written:

assumptions : $T_{\text{RS}} \gg T_{\text{spin}} \gg T_{\text{sky}}$

$$\begin{aligned} (1) \quad T_A^{\text{on}}(v) &= T_{\text{RS}} e^{-\tau_v} + T_{\text{spin}}(v) (1 - e^{-\tau_v}) & \longrightarrow \frac{T_{\text{RS}} - T_A^{\text{on}}(v)}{T_{\text{RS}}} = 1 - e^{-\tau_v} - \frac{T_{\text{spin}}(v)}{T_{\text{RS}}} (1 - e^{-\tau_v}) \\ (2) \quad T_A^{\text{off}}(v) &= T_{\text{sky}} e^{-\tau_v} + T_{\text{spin}}(v) (1 - e^{-\tau_v}) & T_A^{\text{off}}(v) = T_{\text{sky}} + (T_{\text{spin}} - T_{\text{sky}}) (1 - e^{-\tau_v}) \end{aligned}$$



$$(1) \quad \frac{T_{\text{RS}} - T_A^{\text{on}}(v)}{T_{\text{RS}}} \approx 1 - e^{-\tau_v}$$

$$(2) \quad \Delta T_A^{\text{off}}(v) = \Delta T_{\text{spin}}(v) (1 - e^{-\tau_v})$$

or $T_A^{\text{off}}(v) \approx T_{\text{spin}}(v) (1 - e^{-\tau_v})$

Here, $\Delta T_A^{\text{off}}(v) \equiv T_A^{\text{off}}(v) - T_{\text{sky}} \approx T_A^{\text{off}}$
 $\Delta T_{\text{spin}}(v) \equiv T_{\text{spin}}(v) - T_{\text{sky}} \approx T_{\text{spin}}$

$$(T_{\text{sky}} \approx 3 \text{ K})$$

Hereafter, T_A^{off} and T_{spin} denote ΔT_A^{off} and ΔT_{spin} , respectively.

- **Equivalent Width:**

- ▶ Using the absorption spectrum from the “on-source” observation, we can “approximately” obtain the **“velocity equivalent width.”**

$$\begin{aligned} W_v &= \int dv (1 - e^{-\tau_v}) \\ &\approx \int dv \left[\frac{T_{\text{RS}} - T_A^{\text{on}}(v)}{T_{\text{RS}}} \right] \end{aligned}$$

Note : $W_v = c \int \frac{d\nu}{\nu_{ul}} (1 - e^{-\tau_\nu}) = cW$

For a weak absorption line, this approximation is **a lower limit.**

$$\frac{T_{\text{RS}} - T_A^{\text{on}}(v)}{T_{\text{RS}}} = 1 - e^{-\tau_v} - \frac{T_{\text{spin}}(v)}{T_{\text{RS}}} (1 - e^{-\tau_v}) \leq 1 - e^{-\tau_v}$$

In the optically thin case, we also note that $W_v \approx \int \tau_v dv$.

- **Spin Temperature:**

- ▶ Using the equation (2) in the previous page, we can obtain two spin temperatures. The first one is the line-of-sight average spin temperature, and the second the spin temperature in a velocity channel.

$$\langle T_{\text{spin}} \rangle \approx \frac{\int T_A^{\text{off}}(v) dv}{\int (1 - e^{-\tau_v}) dv} = \frac{\int T_A^{\text{off}}(v) dv}{W_v}$$



assuming $T_{\text{spin}} = \text{constant}$.

$$\int dv [T_A^{\text{off}}(v)] = T_{\text{spin}} \int dv (1 - e^{-\tau_v})$$

$$T_{\text{spin}}(v) = \frac{T_A^{\text{off}}(v)}{(1 - e^{-\tau_v})}$$

For a weak absorption line, this T_{spin} is a lower limit.

- ***In an optically thin limit,***

- We know the relation between the antenna temperature and column density:

$$N_{\text{HI}} = C_0 \int [T_A^{\text{off}}(v) - T_{\text{sky}}]$$

$$\approx C_0 \int T_A^{\text{off}}(v) dv$$

$$\frac{dN_{\text{HI}}}{dv} \approx C_0 T_A^{\text{off}}(v)$$

- Then, we can express the spin temperature in terms of column density and equivalent width (absorption profile):

$$\langle T_{\text{spin}} \rangle = \frac{1}{W_v} \int T_A^{\text{off}}(v) dv = \frac{C_0^{-1}}{W_v} N_{\text{HI}}$$

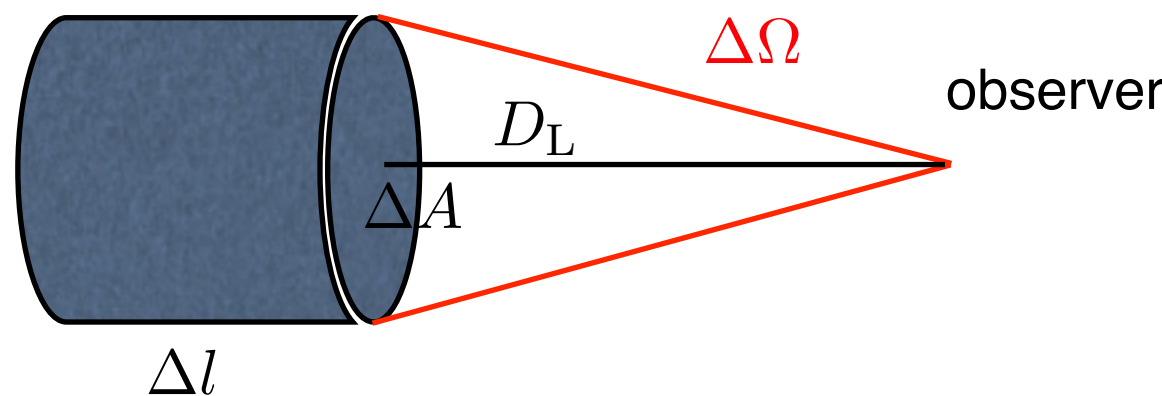
$$\langle T_{\text{spin}} \rangle \approx 0.5516 \frac{N_{\text{HI}}/10^{18} \text{ cm}^{-2}}{W_v/\text{km s}^{-1}} [\text{K}]$$

$$T_{\text{spin}}(v) = \frac{C_0^{-1}}{(1 - e^{-\tau_v})} \frac{dN_{\text{HI}}}{dv}$$

$$C_0^{-1} = 5.516 \times 10^{-19} \left[\frac{\text{K km s}^{-1}}{\text{cm}^{-2}} \right]$$

H I mass of an External Galaxy

- With the assumption that the emitting regions are optically thin, the total mass M_{HI} of H I in an external galaxy can be determined from the observed flux in the 21-cm line:



$$\begin{aligned} F_\nu &= \text{observed flux density} \\ F_{\text{obs}} &= \int F_\nu d\nu_{\text{obs}} = I \Delta\Omega \quad \leftarrow \cos\theta \approx 1 \\ I &= \int I_\nu d\nu_{\text{obs}} = \frac{3}{16\pi} A_{u\ell} h \nu_{u\ell} N_{\text{HI}} \\ I_\nu &= \int j_\nu ds \end{aligned}$$

- Here, D_L is the luminosity distance to the galaxy.

$$n_{\text{H}} \Delta l = N_{\text{HI}}$$

$$\Delta A = D_L^2 \Delta\Omega = D_L^2 \frac{F_{\text{obs}}}{I}$$

$$\begin{aligned} M_{\text{HI}} &= m_{\text{H}} n_{\text{H}} \Delta V = m_{\text{H}} n_{\text{H}} \Delta l \Delta A \\ &= m_{\text{H}} N_{\text{HI}} D_L^2 \frac{F_{\text{obs}}}{I} \\ &= m_{\text{H}} N_{\text{HI}} D_L^2 \frac{F_{\text{obs}}}{(3/16\pi) A_{u\ell} h \nu_{u\ell} N_{\text{HI}}} \end{aligned}$$

The luminosity distance is defined by the relationship between flux and luminosity:

$$F = \frac{L}{4\pi d_L^2}$$

$$\begin{aligned} \therefore M_{\text{HI}} &= \frac{16\pi}{3} \frac{m_{\text{H}}}{A_{u\ell} h \nu_{u\ell}} D_L^2 F_{\text{obs}} \\ &= 4.945 \times 10^7 M_{\odot} \left(\frac{D_L}{\text{Mpc}} \right)^2 \left(\frac{F_{\text{obs}}}{\text{Jy MHz}} \right) \end{aligned}$$

-
- If the redshift of the galaxy is z :

$$\nu_{\text{obs}} = \nu / (1 + z) \quad \longleftrightarrow \quad z = \frac{\nu_{\text{obs}} - \nu_0}{\nu_0}$$

$$d\nu_{\text{obs}} = \frac{\nu_{u\ell}}{(1 + z)} \frac{dv}{c}$$

$$\begin{aligned} M_{\text{HI}} &= \frac{16\pi}{3} \frac{m_{\text{H}}}{A_{u\ell} h \nu_{u\ell}} D_{\text{L}}^2 \int F_{\nu} d\nu_{\text{obs}} \\ &= \frac{16\pi}{3} \frac{m_{\text{H}}}{A_{u\ell} h \nu_{u\ell}} D_{\text{L}}^2 \frac{\nu_{u\ell}}{c} \frac{1}{1+z} \int F_{\nu} dv \\ &= \frac{16\pi m_{\text{H}}}{3 A_{u\ell} h c} D_{\text{L}}^2 (1+z)^{-1} \int F_{\nu} dv \\ &= 2.343 \times 10^5 M_{\odot} (1+z)^{-1} \left(\frac{D_{\text{L}}}{\text{Mpc}} \right)^2 \frac{\int F_{\nu} dv}{\text{Jy km s}^{-1}} \end{aligned}$$

- Radio astronomers often report the integrated flux in “Jy km s⁻¹.”

Observations: Example 1

- All-sky map of H I 21-cm line intensity from the LAB survey (Kalberla et al. 2005), with an angular resolution ~ 0.6 deg.
- Scale gives $\log_{10} N(\text{HI}) [\text{cm}^{-2}]$. The LMC and SMC are visible, with a connecting H I “bridge”.
- The map was obtained by assuming the optically thin case.

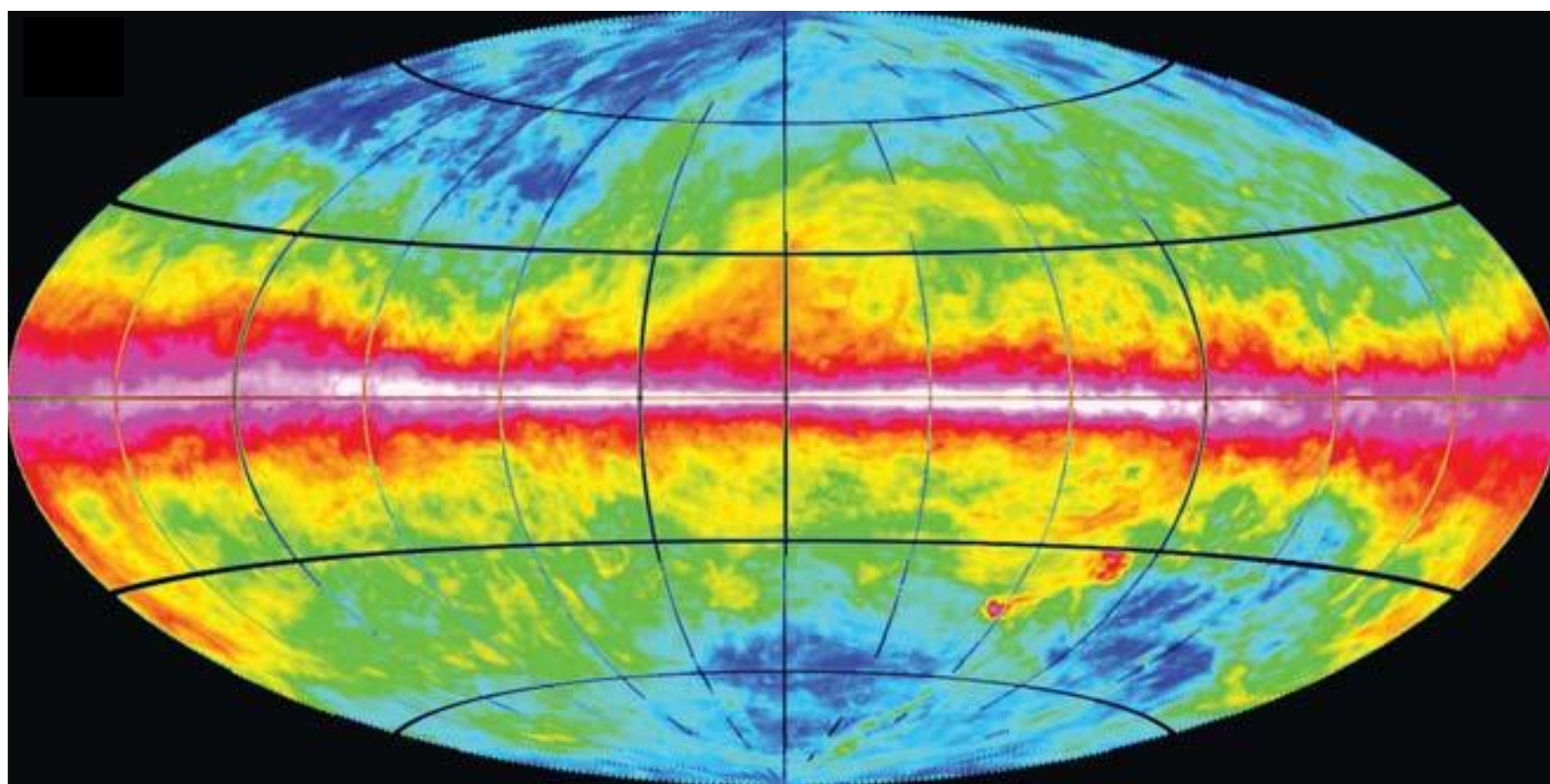
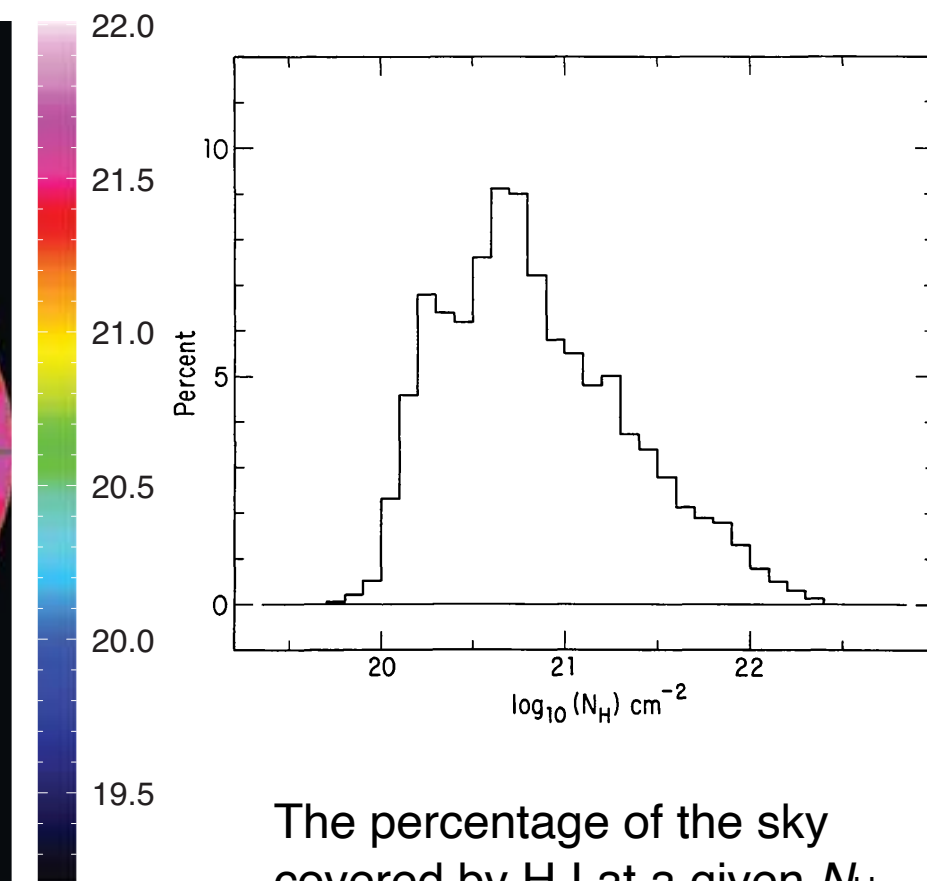


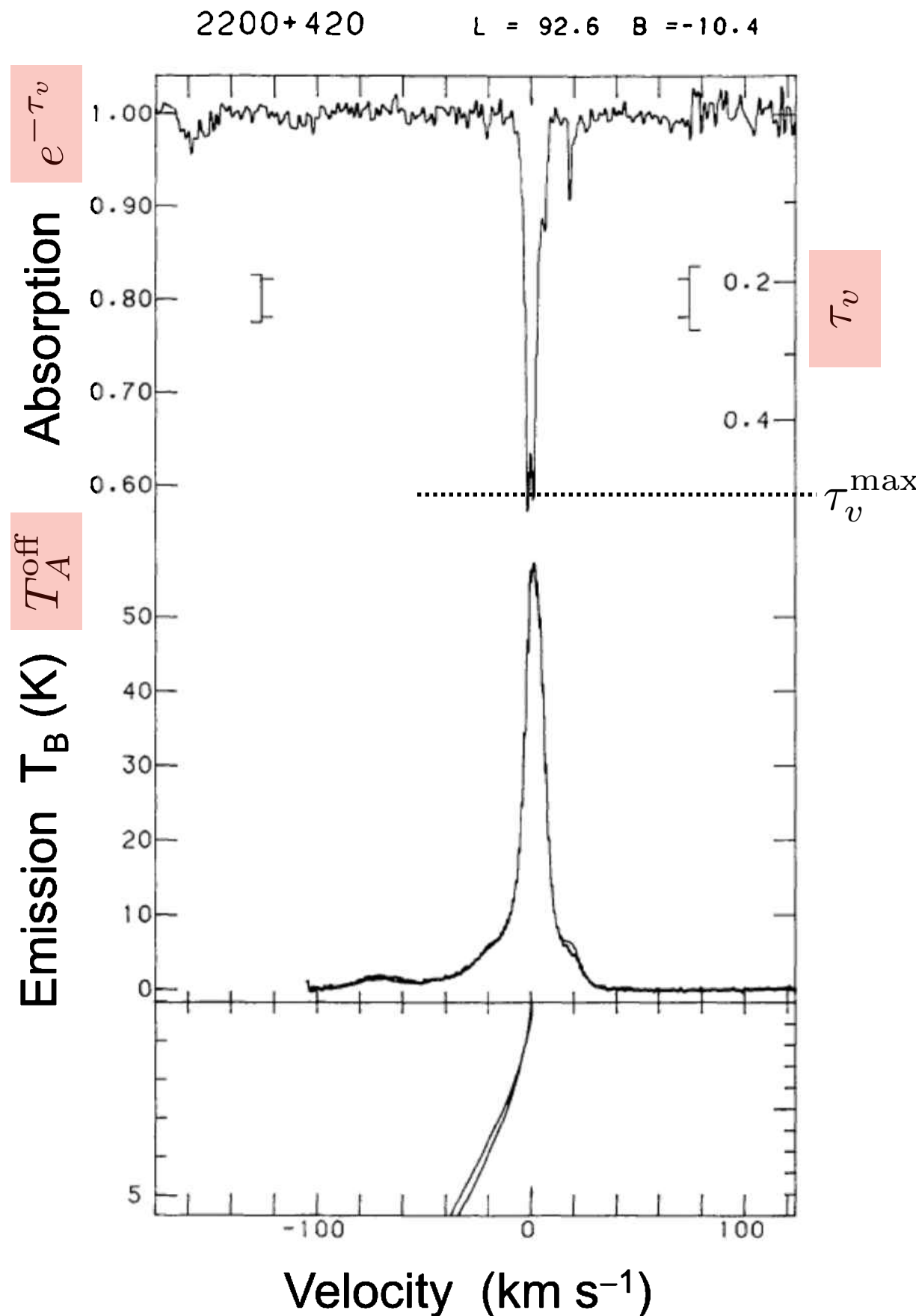
Plate 3 in [Draine]



The percentage of the sky covered by H I at a given N_{H} .

Figure 4 in Dickey & Lockman (1990, ARA&A)

Observations: Example 2



H I 21-cm absorption and emission along the line of sight towards BL Lacertae
[Dickey et al. 1983; Figure 3.3 in Ryden]

[Absorption spectrum]

- Maximum optical depth :

$$\tau_v \sim 0.5 \quad \text{optically thin}$$

- Equivalent width of the absorption line :

$$W_v = 7 \text{ km s}^{-1}$$

[Emission spectrum]

- Integrated line intensity of the emission line :

$$\int T_A^{\text{off}}(v) dv \approx 930 \text{ K km s}^{-1}$$

- Column density from the emission line :

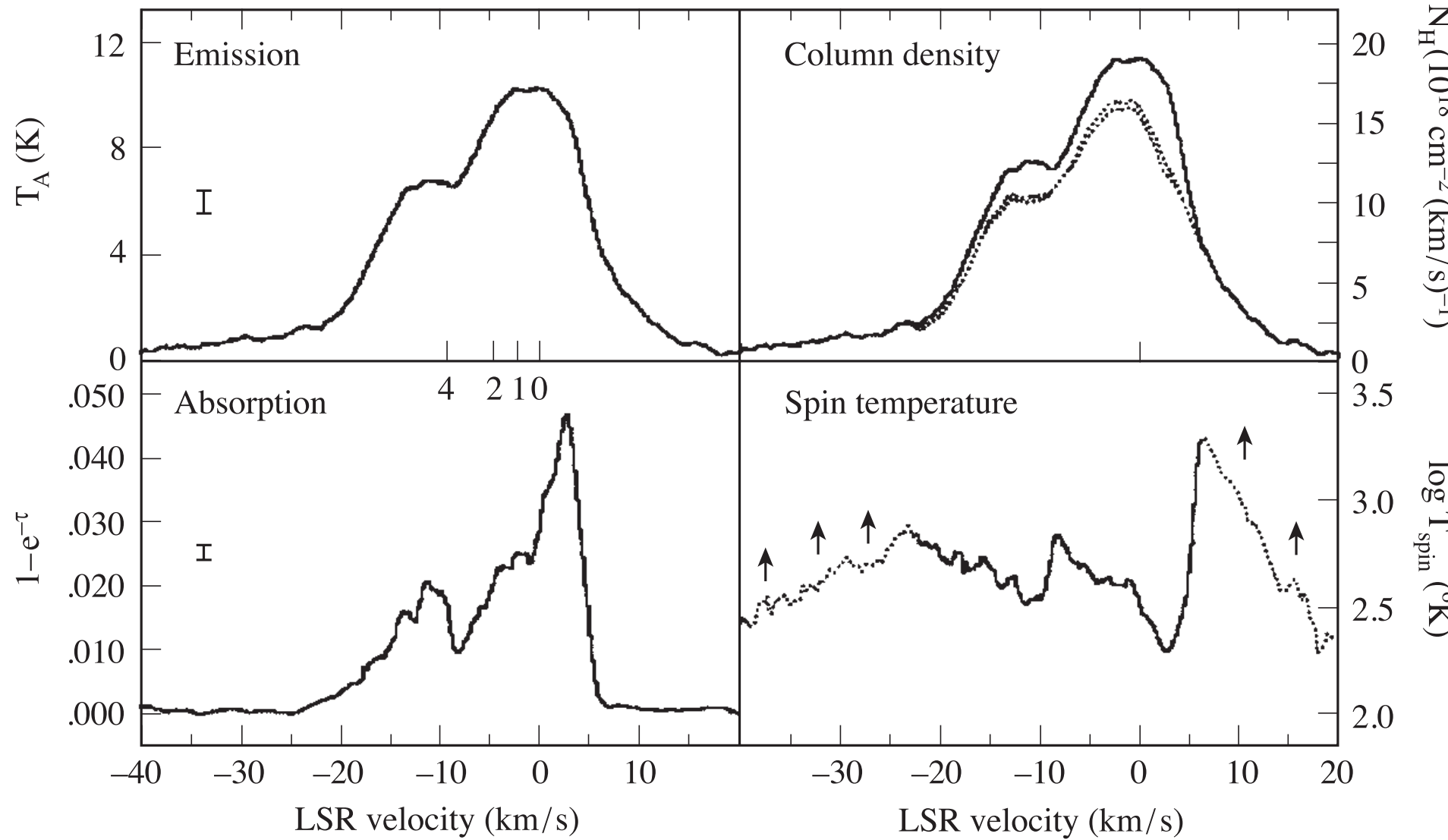
$$N_{\text{HI}} \approx 1.69 \times 10^{21} \text{ cm}^{-2}$$

- Now, the spin temperature is

$$T_{\text{spin}} = \frac{\int T_A^{\text{off}}(v) dv}{W_v} = \frac{930 \text{ K km s}^{-1}}{7 \text{ km s}^{-1}}$$

$$\approx 133 \text{ K.}$$

Observations: Example 3



Left panels: Observed HI emission (off the quasar 3C48) and absorption (toward 3C48, at $\ell = 134^\circ$, $b = -28.7^\circ$). Lower right: spin temperature $T_{\text{spin}}(v)$ as a function of LSR velocity. Tick marks labeled 0, 1, 2, and 4 on abscissa of left panels show the LSR velocity expected for gas at a distance of 0, 1, 2, 4 kpc (for an assumed Galactic rotation curve). Upper right: $dN(\text{HI})/dv$ for different assumptions regarding the relative (foreground/background) locations of cold absorbing gas and warm gas seen only in emission. From Dickey et al. (1978).

[Figure 29.1 in Draine]

Define a point in space that is moving on a perfectly circular orbit around the center of the Galaxy at the Sun's galactocentric distance.

We measure all velocities of astronomical objects relative to this point, which is the **LSR (local standard of rest)**.

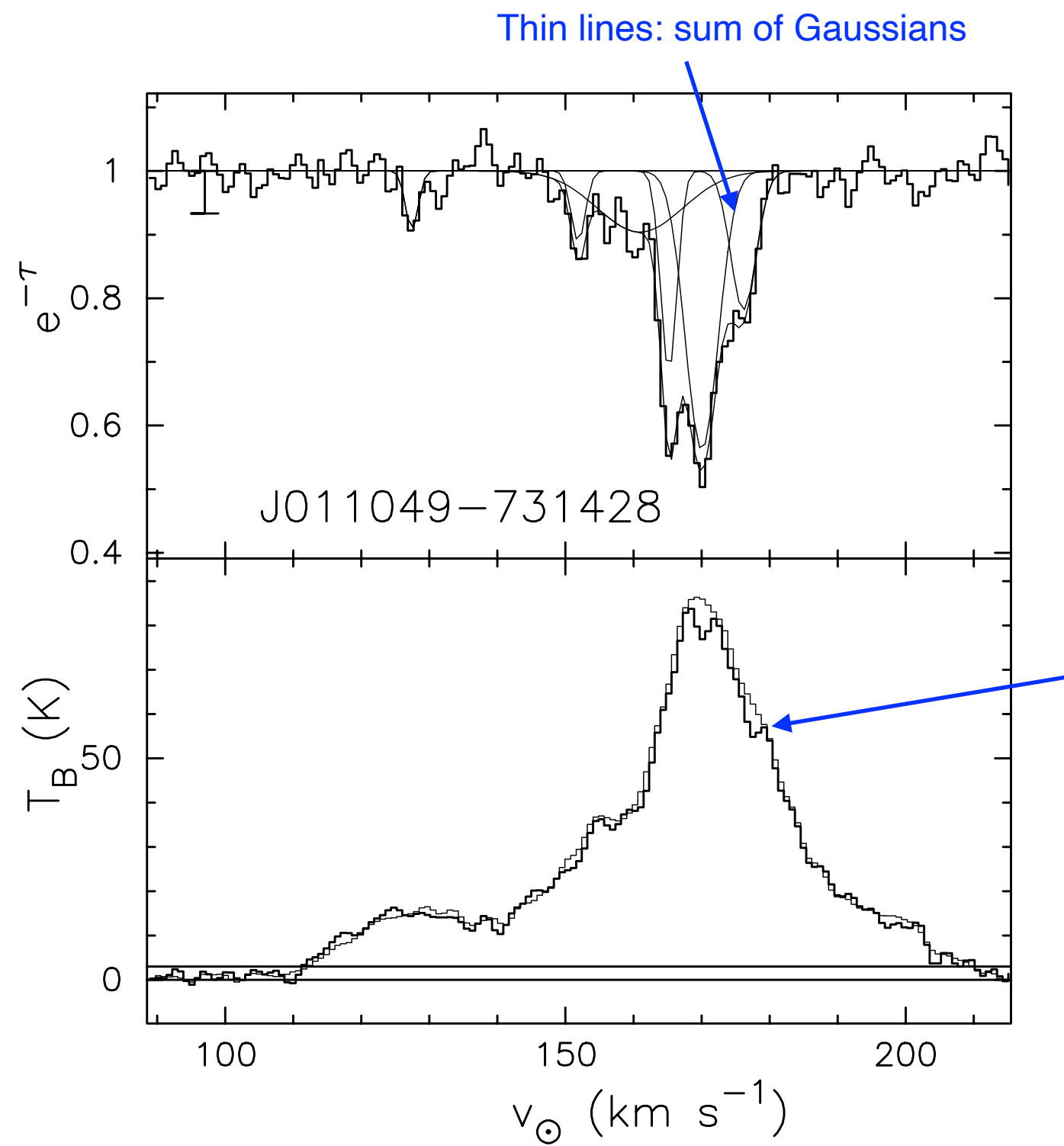
The Sun's orbital speed is 202-241 km/s (Majewski 2008, IAUS, 248).

Observations: CNM & WNM

- The overall shape of the emission line profiles in our Galaxy is mainly determined by the large-scale distribution and kinematics of H I.
- Absorption lines are always narrower than emission lines.
 - Some velocities have H I emission but no detectable H I absorption.
 - Difference between emission and absorption spectrum:
 - ▶ Absorption spectra can usually be decomposed into Gaussian components.
 - ▶ However, emission spectra do not look like the superposition of a few Gaussians.
 - ▶ This is because the absorption lines arise only in regions of cool gas, which are more distinct along the line of sight, and thus have narrower intrinsic line widths than the gas that contributes to H I emission.
- The difference between emission and absorption results mainly from variation in the spin temperature of the H I along the line of sight.
 - Recall that the optical depth is inversely proportional to the spin temperature, indicating the difficulties in observing absorption spectra from the warm neutral medium, which has a temperature larger than 1000 K.

$$\tau(v) = \frac{C_0^{-1}}{T_{\text{spin}}(v)} \frac{dN_{\text{HI}}}{dv}$$

- Absorption and Emission spectra



Absorption lines are mostly, if not all, caused by the CNM.

$$\tau(v) = \frac{C_0^{-1}}{T_{\text{spin}}(v)} \frac{dN_{\text{HI}}}{dv}$$

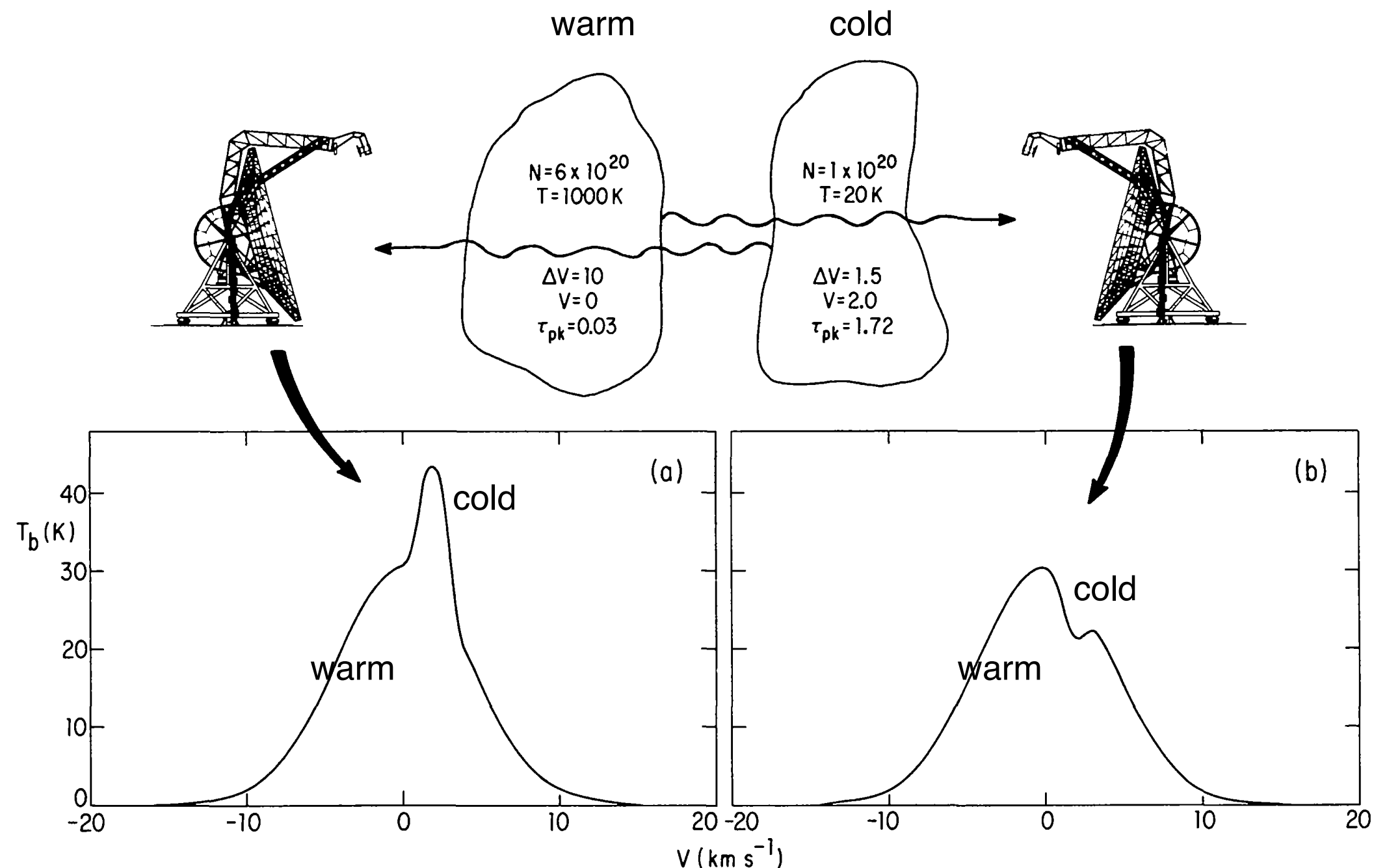
Emission lines are composed of emissions from the CNM and WNM.

Thin and Thick lines:
two different methods to
estimate the emission
spectrum

(top) Absorption and (bottom) emission
spectra in a direction of Small Magellanic
Cloud.

Figure 11 of Dickey et al. (2000)

Emission spectrum depending on the relative location of WNM and CNM



[Schematic of the geometry of 21-cm self-absorption]

The structure of an emission profile depends on the relative location of warm and cold clouds as viewed by the observer.

Figure 1 of Dickey & Lockman (1990)

A rough estimation of the fraction of gas in the cold phase

- The interstellar atomic hydrogen is in at least two thermal phases.
 - We assume that the warm gas temperature is large enough that no absorption is seen from the warm phase.
 - We further assume a value for the cold-phase temperature, for instance, $T_c \approx 55 \text{ K}$.

- Then, the fraction of gas in the cold phase is

$$f_c \equiv \frac{N_c}{N_w + N_c} \approx \frac{T_c}{\langle T_{\text{spin}} \rangle}$$

$$T_c = \frac{C_0^{-1}}{W_v^c} N_c$$

$$\langle T_{\text{spin}} \rangle = \frac{C_0^{-1}}{W_v} N_{\text{HI}}, \text{ where } W_v = W_v^c + W_v^w \approx W_v^c \text{ and } N_{\text{HI}} = N_w + N_c$$

The warm gas and cool gas are mixed so that T_{spin} is a weighted average, whether computed for individual velocity channels or line-of-sight integrals.

- This gives us a rough estimation of the cold-phase H I fraction for galaxies.

Cool-Phase H I Fractions for Galaxies

Galaxy	Sample Size	$\langle T_s \rangle$ (K)	f_c ($T_c = 55 \text{ K}$)
SMC	28	440	0.13
LMC	49	170	0.33
M31	16	150	0.37
M33	7	370	0.15
Milky Way.....	19	250	0.22

Observations: CNM + WNM in our Galaxy

- The emission-absorption surveys (Heiles & Troland 2003) support the idea that, in the solar neighborhood (i.e., within ~ 500 pc of the Sun), interstellar H I is found primarily in two distinct phases: the CNM and the WNM.
 - About 40% of the H I (by mass) is in the CNM, with a median spin temperature $T_{\text{spin}} \sim 70$ K. The remaining 60% of the H I is in the WNM phase, which appears to have a volume filling factor $\sim 50\%$ near the disk midplane.
 - Because warm H I absorbs very weakly, for some of the WNM material, it is only possible to determine a lower bound on T_{spin} . Heiles & Troland (2003) conclude that $> 48\%$ of the WNM has $500 < T_{\text{spin}} < 5000$ K, at these temperatures the gas is expected to be thermally unstable.
- Murray et al. (2014) detected a widespread warm neutral medium component with excitation temperature $\langle T_{\text{spin}} \rangle = 7000^{+1800}_{-1200}$ K.
 - This temperature lies above theoretical predictions based on collisional excitation alone, implying that Ly α scattering, the most probable additional source of excitation, is more important in the ISM than previously assumed.
- Murray et al. (2018) found that the WNM makes up 52% of the total H I mass.
 - Following spectral modeling, they detect a stacked residual absorption feature corresponding to WNM with $T_{\text{spin}} \sim 10^4$ K.

Excitation temperature = Gas kinetic temperature ?

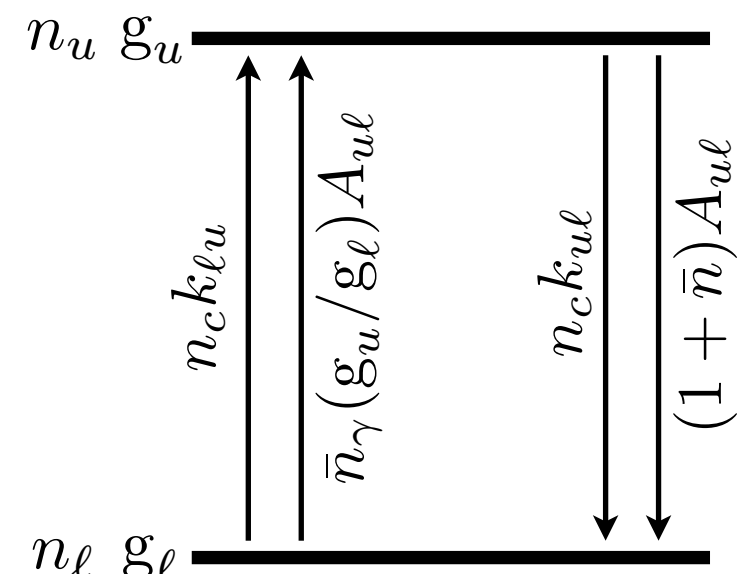
- In some cases, it is sufficient to consider only the ground state and the first excited state.
 - Consider collisional excitation and de-excitation by some species (e.g., electrons) with density n_c , and suppose that radiation with the energy density u_ν .
 - The population of the excited state must satisfy:

$$\frac{dn_u}{dt} = n_\ell \left[n_c k_{\ell u} + \bar{n}_\gamma \frac{g_u}{g_\ell} A_{u\ell} \right] - n_u \left[n_c k_{u\ell} + (1 + \bar{n}_\gamma) A_{u\ell} \right]$$

- The steady-state solution with radiation and collision present is

$$\frac{n_u}{n_\ell} = \frac{n_c k_{\ell u} + \bar{n}_\gamma (g_u/g_\ell) A_{u\ell}}{n_c k_{u\ell} + (1 + \bar{n}_\gamma) A_{u\ell}}$$

$$\frac{n_u}{n_\ell} = \frac{g_u}{g_\ell} \exp(-E_{u\ell}/k_B T_{\text{exc}})$$



Here, photon occupation number
 $\left(\bar{n}_\gamma \equiv \frac{c^3}{8\pi h\nu^3} u_\nu \right)$

By combining these two equations, we can calculate the excitation temperature between the two levels.

Here, by the principle of detailed balance, the upward collisional rate coefficient is given in term of the downward rate coefficient by

$$k_{\ell u} = \frac{g_u}{g_\ell} k_{u\ell} e^{-E_{u\ell}/kT_{\text{gas}}} \quad (T_{\text{gas}} = \text{gas kinetic energy})$$

Excitation Temperature - Limiting Cases

- It is instructive to examine the population equation in various limits:

- In the limit of $n_c \rightarrow \infty$ and no or weak radiation field $\bar{n}_\gamma = 0$:

$$\frac{n_u}{n_\ell} = \frac{n_c k_{\ell u}}{n_c k_{u\ell} + A_{u\ell}} = \frac{k_{\ell u}}{k_{u\ell}} = \frac{g_u}{g_\ell} e^{-E_{u\ell}/kT_{\text{gas}}} \quad \therefore T_{\text{exc}} = T_{\text{gas}}$$

- If $n_c = 0$ and the radiation field has a brightness temperature of $T_b = T_{\text{rad}}$ at the frequency $\nu = E_{u\ell}/h$:

$$\frac{n_u}{n_\ell} = \frac{\bar{n}_\gamma(g_u/g_\ell)}{(1 + \bar{n}_\gamma)} = \frac{g_u}{g_\ell} e^{-E_{u\ell}/kT_{\text{rad}}} \quad \therefore T_{\text{exc}} = T_{\text{rad}}$$



$$\bar{n}_\gamma = \left(e^{E_{u\ell}/kT_{\text{rad}}} - 1 \right)^{-1} \implies 1 + \bar{n}_\gamma = \bar{n}_\gamma e^{E_{u\ell}/kT_{\text{rad}}}$$

- If the radiation and gas has the same temperature $T_{\text{rad}} = T_{\text{gas}}$, then we can show that

$$\frac{n_u}{n_\ell} = \frac{n_c k_{\ell u} + \bar{n}_\gamma(g_u/g_\ell)A_{u\ell}}{n_c k_{u\ell} + (1 + \bar{n}_\gamma)A_{u\ell}} = \frac{g_u}{g_\ell} e^{-E_{u\ell}/kT_{\text{gas}}} \quad \therefore T_{\text{exc}} = T_{\text{rad}} = T_{\text{gas}}$$

- In general, $T_{\text{exc}} \neq T_{\text{gas}}$ and $T_{\text{exc}} \neq T_{\text{rad}}$. What is the excitation temperature in the ISM?

Critical Density

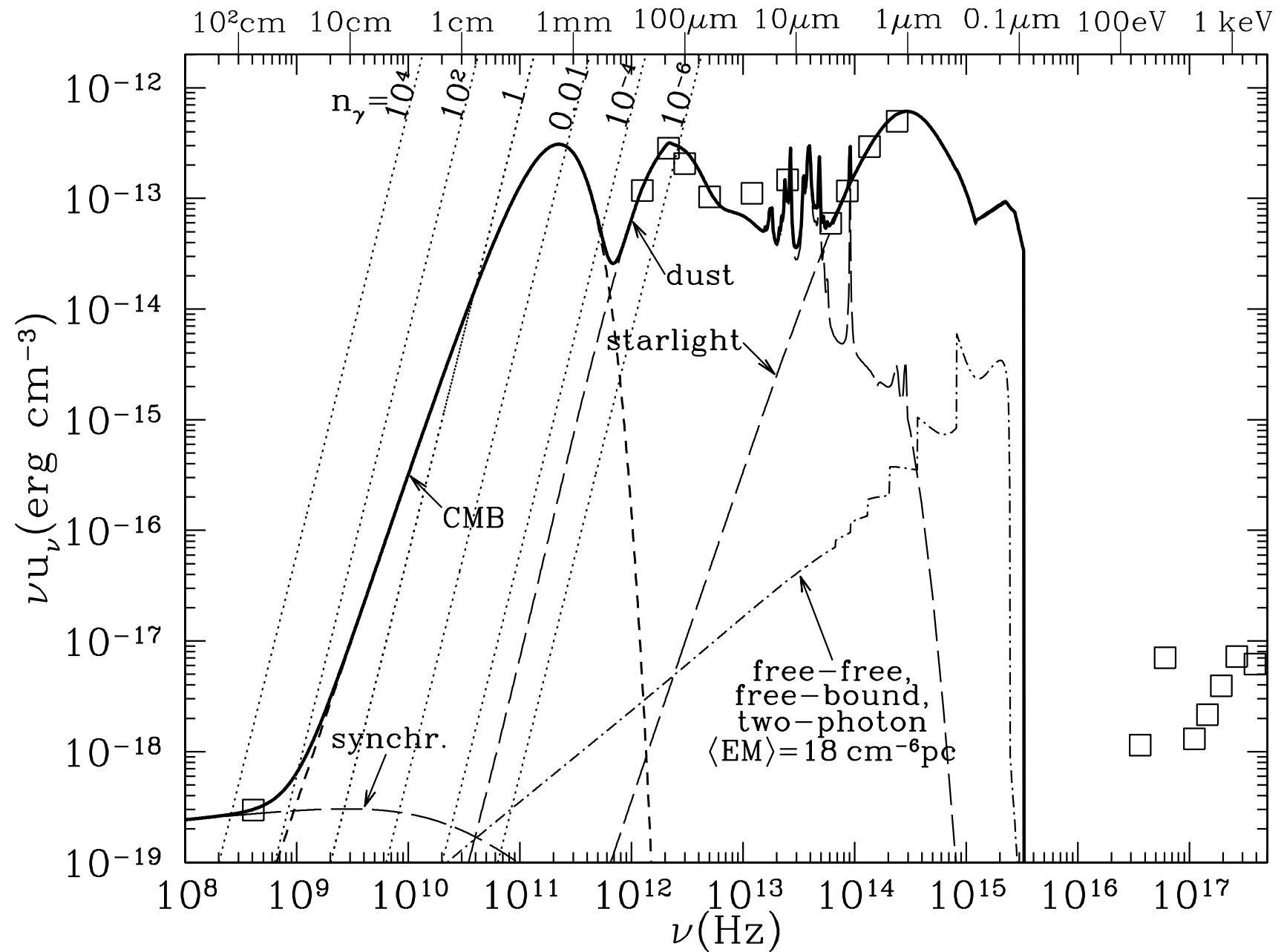
- Interplay between the radiation and collisions determines the excitation temperature. Which one will be more important?
 - For a collision partner c , we define the critical density $n_{\text{crit}, u}$ for an excited state u to be the density for which collisional de-excitation equals radiative de-excitation, including stimulated emission:
- $$n_{\text{crit}, u}(c) \equiv \frac{\sum_{\ell < u} [1 + (n_\gamma)_{u\ell}] A_{u\ell}}{\sum_{\ell < u} k_{u\ell}(c)}$$
- Note that this definition applies to multilevel systems, but each excited level u may have a different critical density. The critical density depends on the intensity of ambient radiation. For many transitions, the correction by the stimulated emission is unimportant, but for 21-cm line, it is important.

Critical densities for fine-structure excitation [Table 17.1 in Draine, revised for both H and e^- , errata]

Ion	ℓ	u	E_ℓ/k	E_u/k	$\lambda_{u\ell}$	$n_{\text{crit}, u}(\text{H})$	$n_{\text{crit}, u}(e^-)$
			(K)	(K)	(μm)	$T = 100 \text{ K}$ (cm^{-3})	$T = 5000 \text{ K}$ (cm^{-3})
C II	$^2\text{P}_{1/2}^o$	$^2\text{P}_{3/2}^o$	0	91.21	157.74	2.7×10^3	1.5×10^3
	$^3\text{P}_0$	$^3\text{P}_1$	0	23.60	609.7	620	170
CI	$^3\text{P}_1$	$^3\text{P}_2$	23.60	62.44	370.37	720	150
	$^3\text{P}_2$	$^3\text{P}_1$	0	227.71	63.185	2.5×10^5	4.9×10^4
OI	$^3\text{P}_1$	$^3\text{P}_0$	227.71	326.57	145.53	2.4×10^4	8.6×10^3
	$^3\text{P}_2$	$^3\text{P}_1$	0	227.71	63.185	1.2×10^5	1.8×10^5
Si II	$^2\text{P}_{1/2}^o$	$^2\text{P}_{3/2}^o$	0	413.28	34.814	4.8×10^4	2.8×10^4
	$^3\text{P}_0$	$^3\text{P}_1$	0	110.95	129.68	9.9×10^4	4.4×10^4
Si I	$^3\text{P}_1$	$^3\text{P}_2$	110.95	321.07	68.473	$140.$	$830.$
							1.9×10^3

Interstellar Radiation Fields

To estimate the critical density, we need to know the radiation field strength.



Interstellar continuum radiation field in an HI cloud in the solar neighborhood (see text). Spectral lines are not included. Solid line is the sum of all components for $h\nu \leq 13.6$ eV. Squares show the measured sky brightness at 408 MHz (Haslam et al. 1982), the all-sky measurements by COBE-DIRBE in 10 broad bands from $240\text{ }\mu\text{m}$ to $1.25\text{ }\mu\text{m}$ (Arendt et al. 1998), and all-sky measurements by ROSAT between 150 eV and 2 keV (Snowden 2005, private communication). Dotted lines are contours of constant photon occupation number n_γ .

[Figure 12.1 in Draine]

Homework (due date: 04/21)

[Q6]

- Measurements of the equivalent width of the absorption Na I D lines at $\lambda = 5890\text{\AA}$ in the direction of star HD 190066 (type B1I) give the result $W \sim 400 \text{ m\AA}$.
- (1) Assume this is a weak line and calculate the column density of neutral Na atoms in the direction of the star. Show that in this case, the following relation is valid:

$$N \simeq \frac{11.3 (W_\lambda / \text{m\AA})}{(\lambda / \text{cm})^2 f_{u\ell}} [\text{cm}^{-2}]$$

Here, use $f_{u\ell} = 0.65$.

- (2) Analysis of the line saturation suggests a correction factor of 6 for the column density. Apply this factor to the above result and estimate the Na total column density, assuming that 99% of the sodium atoms are ionized.

[Q7]

A dwarf galaxy at a distance $D_L = 15 \text{ Mpc}$ is emitting in the 21-cm line of atomic hydrogen. The observed 21-cm line flux is $F = 1 \times 10^{-8} \text{ erg cm}^{-2} \text{ s}^{-1}$.

If the emitting gas is assumed to be optically thin, and there is no absorption by intervening gas, estimate the mass of H I in the dwarf galaxy. Express your answer in solar mass M_\odot .

The Einstein A coefficient for the 21-cm line is $A_{ul} = 2.88 \times 10^{-15} \text{ s}^{-1}$.